CA16-013

PN. ACH-644

104874

ANNUAL REPORT

Covering Period: 1.01.1999-31.12.1999

Protection of land and settlements in arid regions from contamination by atmospheric deposition

Principal Investigator:	Arieh Singer
Co-Investigators:	Yitzhak Mahrer and Amos Banin
Grantee Institution:	The Hebrew University of Jerusalem

Collaborators:	Dr. L. Poberezsky
	Dr. M. Gilenko
Institution:	Scientific Research Association
	"Waterproject", Victor Malaysov Str. 3
	Tashkent 7000, Uzbekistan

MAR 15 2000

AID/CDR

Grant Number: TA-MOV-96-CA16-013

(030-6194)

A

PN-ACH-644

ANNUAL REPORT

Covering Period: 1.01.1999-31.12.1999

Submitted to the Office of Agriculture & Food Security
U.S. Agency for International Development

Protection of land and settlements in arid regions from contamination by atmospheric deposition

Principal Investigator:	Arieh Singer
Co-Investigators:	Yitzhak Mahrer and Amos Banin
Grantee Institution:	The Hebrew University of Jerusalem

Collaborators:	Dr. L. Poberezsky
	Dr. M. Gilenko
Institution:	Scientific Research Association
	"Waterproject", Victor Malaysov Str. 3
	Tashkent 7000, Uzbekistan

Project Number:	
Grant Number:	**TA-MOV-96-CA16-013**

Grant Project Officer:	Mr. David Mulenex
	Science Attache, U.S. Embassy
	Tel-Aviv, Israel.

Project Duration:	January 1, 1997 – December 31, 2000

B

TABLE OF CONTENTS

	Page
Table of Contents	1
Executive Summary	2
SECTION I	
A) Research Objectives	4
B) Research Accomplishments	4
(1) Representation and analysis of data using the GIS System	4
Figs. 1-12: GIS maps	12
(2) Meteorological model for dust transfer and deposition	24
Dust propagation following desiccation of the Aral Sea	24
Graphic representations of model maps	32
(3) Meteorological and soil data of the Aral Sea region	36
Wind conditions in the Aral region	36
Protection of industrial objects of Kungrad district from Harmful action of atmospheric depositions	51
C) Scientific Impact of Collaboration	57
D) Description of Project Impact	57
E) Strengthening of Developing Country Institutions	57
F) Future Work	58
SECTION II	
A and B)	58
D) Collaboration during 1999	58

EXECUTIVE SUMMARY

The purpose of this research is to provide recommendations for the establishment of measures aimed at containing the process of salt transfer, propagation and deposition in the Amu Darai River delta, southern Aral Sea. A comprehensive approach has been taken so that the recommendations will be based on an analysis of ground data using the GIS system, on devising a mathematical model that would describe, quantify and predict the processes of atmospheric salt transport and on an examination of methods for the reduction of dust generation by soil surface stabilization.

During the third project year (1999), the GIS database, containing information on land use and management, salinity, texture and hydromorphism of the Amu Darai River delta, were used to create superpositions for the purpose of analysis and interpretation of the data. Detailed analysis was carried out for two strategic areas, Chimbay and Kungrad, where urban and industrial development is planned. This work was carried out using the PC that was purchased for the Uzbek partners in 1998.

Using updated data on the wind activity in the Aral Sea region, the Uzbek partners analyzed the wind regime characteristics in the Aral Sea region. This analysis is important for the deflatability studies to be carried out in the wind tunnel in Israel. Also in preparation for these studies, the Uzbek partners prepared an assessment of the soil surfaces that may serve as sources for dust entrainment. In this study, the changes in the moisture regime of Solonchak and Hydromorphic soils throughout the year are detailed. As a result of these studies, recommendations for the management of these lands were formulated.

Prof. Y. Mahrer participated in an international workshop on "Mineral Dust" held in Boulder, Colorado, in June 1999, and presented there a paper on the application of a three-dimensional numerical model to dust generation and transport in the Aral Sea region. Prof. Singer participated in an international workshop on "Desert Ecosystems", held in Germany in May 1999. He presented there a paper on crust formation in the Aral region soils. Contacts with other research groups were established.

The equipment required for the wind tunnel tests to be carried out on soils from the Amu Darai River delta was purchased. Preliminary tests on model soils were carried out.

The two principal collaborators of the project visited Israel twice in the course of 1999 for discussions on the results so far obtained, and on plans for future work.

The plan for the year 2000 (project duration extension of one year) consists principally in the examination of dust entrainment from samples of the 4 soils that were brought from

Uzbekistan, using a wind tunnel. The effects of chemical treatments and of other parameters (moisture, crusts) on deflatability, will be tested as well. Two or three additional samples of soils/sediments from the Aral Sea area will be made available in the course of 2000.

Work on the dust propagation model will be continued as well. Specifically, the effects of continued desiccation, as against recovery of the Aral Sea, will be examined.

SECTION I

SIGNIFICANT SCIENTIFIC RESULTS

A) Research Objectives

(a) To collect the data essential for an assessment of the phenomenon of atmospheric salt transfer and deposition in the Aral Sea area, and analyze the data using the GIS system.

(b) To assess the rate of mineral (aluminosilicates, soluble salts) matter deflation and deposition taking place in the specified area.

(c) To devise a meteorological model that would describe, quantify, and predict the processes of salt transport and deposition. To establish a salt balance for the region.

(d) To examine methods for the reduction of soil deflation and dust generation by soil surface stabilization, using treatments with soil stabilizers.

(e) To provide recommendations for the establishment of measures aimed at containing the process of salt transfer, propagation and deposition. More specifically: (a) To provide recommendations related to plans for the construction of artificial water bodies/reservoirs, and predict their eventual effects on the process of dust transfer/deposition, using a numerical model; (b) To assess the effect of soil-surface stabilization on regional dust transfer.

B) Research Accomplishments

(1) Representation and analysis of data using the GIS system.

Research objectives

To collect the data essential for an assessment of the phenomenon of atmospheric salt transfer and deposition in the Aral Sea area, and analyze the data using the GIS system.

General

Based on the GIS cartographic data including soil types, salinities, textures, hydromorphism, land management and land use, super-positions of the respective layers were created, yielding important results, presented below in Tables 1-9.

Table 1 gives the areas of 5 soil type groups, as obtained from the Amu Darai delta soil map. The 25 soil types (that were presented in the 1997 report) were condensed into 5 principal groups: Hydromorphic soils, Takyrs, Solonchaks, Sands, and Gray soils. There is a certain overlap between Hydromorphic soils and Solonchaks.

Table 1. Areas of the principal soil type groups in the Amu Darai River delta.

Soil type group	Area (polygons)	Units (m^2)
Hydromorphic soils	1206	5.18×10^9
Takyrs	477	2.61×10^9
Sands	149	5.47×10^8
Solonchaks	50	1.85×10^8
Gray soils	23	0.85×10^8
Other areas	262	1.13×10^8

This table indicates that about 2/3 of the soils are affected by hydromorphism, i.e. are not drained; most of these soils are also saline: another large group are the Takyrs, that exhibit surface crusting, but are only mildly saline. Solonchak soils, as well as some of the hydromorphic soils, exhibit salt crusting.

Table 2 grades the major soil type groups according to their salinity status. Five salinity grades were defined: 0 – very low salinity; 1 – lightly saline (<0.2%); 2 – moderately saline (0.2-0.5%); 3 – strongly saline (0.5-2%); 4 – very strongly saline (>2%); data for soil salinity were taken from existing Uzbek literature.

Table 2. Soil types of the Amu Darai River delta and their average salinities. GIS super-position of soil salinity over soil type.

Soil type	Extent (polygons)	Ave. salinity	Min. salinity	Max. salinity
Takyrs	10	2.1	1	3
Solonchaks	3	3	3	3
Hydromorphic Soils	17	2.3	1	4
Gray soils	2	2.5	2	3
Sands	1	0	0	0
Unmapped	2	0	0	0

This table indicates that only sands are not afflicted by salinity. The highest salinity is exhibited by some hydromorphic soils. These would probably qualify for the definition of Solonchaks. Other hydromorphic soils are only slightly saline. The most consistently saline soils are the Solonchaks. Takyrs and gray soils are only mildly saline.

Table 3 examines the relation between the texture of soils and their salinity status. Soil texture was defined in grades between sandy and heavy clay. No equivalent of loamy texture (in the USDA) was found in the Russian classification. Mixed textures are soils where sandy material is interlayered in clay-rich soils.

Table 3. Soil texture of the Amu Darai River delta soils and their salinity state. GIS super-position of salinity state over soil texture.

Soil texture	Extent (polygons)	Ave. salinity	Min. salinity	Max. salinity
No defined texture	2	0	0	0
Sandy	2	1	0	2
Light clay	10	2	1	4
Moderate clay	8	2	1	3
Heavy clay	8	2.9	1	4
Mixed clay	5	2.6	2	3

Table 3 indicates that light clay soils (probably equivalent to loam or silty loam in the USDA) dominate. The extent of sandy soils is very limited. Only sandy soils are not saline or slightly saline. The heavy soils are the most saline. The soils with mixed texture are quite saline too.

In Table 4, the hydromorphism of the soils in the Amu Darai River delta is superposed on their texture. The hydromorphism is expressed in three grades: 0 – no hydromorphism; 1 – mild hydromorphism; 2 – strong hydromorphism. In grade 2, the soils are water-saturated most of the year, in grade 1, only part of the year.

Table 4. Soil texture of the Amu Darai River delta and their hydromorphic state. GIS superposition of hydromorphic state over soil texture.

Soil texture	Extent (polygons)	Ave. hydromorphism	Min. hydromorphism	Max. hydromorphism
No	2	0.5	0	1
Sandy	2	0	0	0
Light clay	10	1.3	0	2
Moderate clay	8	1	0	2
Heavy clay	8	1.7	1	2
Mixed clay	5	1.6	0	2

Table 4 shows that in sandy soils, hydromorphism does not occur. Hydromorphism is strongest in the heavy clay soils. Also, soils with "mixed" texture are strongly affected by hydromorphism. These relationships are as expected.

In Table 5, the relationship between salinity of soils and their hydromorphic state are represented. Non-saline soils are only slightly hydromorphic. The most saline soils are those with the strongest hydromorphism. This suggests that salinity is strongly associated with water, either rising groundwater or irrigation water. It is also noteworthy that some mildly or even strongly saline soils are not hydromorphous.

Table 5. Saline soils of the Amu Darai River delta and their hydromorphism. GIS superposition of hydromorphic state over soil salinity.

Soil salinity	Extent (polygons)	Ave. hydromorphism	Min. hydromorphism	Max. hydromorphism
0	3	0.3	0	1
1	7	1.4	0	2
2	10	1.1	0	2
3	13	1.4	0	2
4	2	2	2	2

In Table 6, the major land-use types in the Amu Darai River delta are shown, with the salinities of the associated soils. The area covered by these types is much larger than the area of the soil types, since the land use maps were more extensive. Only principal land-use types are indicated.

Table 6. Land use types in the Amu Darai River delta and the salinities of the respective soils. GIS superposition of soil salinity over land use.

Land use	Extent (polygons)	Ave. salinity	Min. salinity	Max. salinity
Cultivated land	9	2.62	2	3
Pasture (natural)	3285	2.30	0	4
Horticulture	224	2.22	0	4
Sands	2387	2.16	0	4
Irrigated fields	148	2.64	0	4
Fields with drainage	34	2.09	0	4
Planted forest trees	58	2.03	0	4
Semi-dry solonchaks	24	1.70	0	3
Rice fields	43	2.14	1	4
Cobbly terrain	29	2.10	0	3
Uncultivated land	363	1.82	0	4

Pasture (natural) takes up the largest area. While some of this pasture land is strongly saline, other lands are salt-free. Sands are also widespread, and are partly hydromorphic. It is remarkable that the land use defined as "cultivated" is, on the average, the most saline. The land use defined as "irrigated fields" probably is drained and is also quite saline. This suggests that cultivation in these environments inevitably leads to salinization.

Table 7 shows land management of Amu Darai River delta lands and the salinities of the respective lands. Land management refers to irrigation, history of irrigation and pasture. This table shows that all irrigated lands and all pasture lands are saline to some degree, while some non-irrigated lands are not saline. The pasture lands are moderately saline, while in the other land all salinity grades are represented.

Table 7. Land management of the Amu Darai River delta and the salinities of the respective lands. GIS superposition of soil salinity over land management.

Land management	Extent (polygons)	Average salinity	Minimum salinity	Maximum salinity
Non-irrigated	18/35	2.2	0	4
Recently irrigated	12/35	2	1	4
Longtime irrigated	4/35	2	1	3
Pasture	1/35	2	2	2

In Table 8, land management is shown as related to texture. This table indicates that while pasture land as a rule is sandy, the irrigated lands are clay textured. It can be deduced that sandy lands were deemed unsuitable for irrigated cultivation.

Table 8. Land management of the Amu Darai River delta and the textures of the respective lands. GIS superposition of land textures over land management.

Land management	Extent (polygons)	Common land texture	Range of land textures
No irrigation	18/35	Light clay	Sandy-heavy clay
Recent irrigation	12/35	Light clay	Light clay-heavy clay
Old Irrigation	4/35	Moderate clay	Light clay-heavy clay
Pasture	1/35	Sandy	Sandy

Table 9 shows land management in the Amu Darai River delta related to hydromorphic state. Pasture land can be seen to be non-hydromorphic, as contrasted with irrigated land, part of which is affected by hydromorphism. Old irrigated land is invariably strongly hydromorphic, while newly-irrigated land is only partly hydromorphic.

Table 9. Land management of the Amu Darai River delta and its hydromorphic state. GIS superposition of hydromorphism over land use.

Land management	Extent (polygons)	Ave. hydromorphism	Min. hydromorphism	Max. hydromorphism
No irrigation	18/35	1.05	0	2
Recently irrigated	12/35	1.42	0	2
Old irrigation	4/35	2	2	2
Pasture	1/35	0	0	0

Fig. 1 shows the desiccation sequence of the Aral Sea between 1957 and 1998.

For GIS representation, two key regions were selected, based on their importance as centers of urban and rural development, and also on the availability of data. The key areas are:

Fig. 2 (1) the area surrounding the town of Chimbay, in the east of the delta (a in Fig. 2) and (2) the area surrounding the town of Kungrad, in the west of the delta (b in Fig. 2). For the area surrounding the town of Muynak (e in Fig. 2), not enough data was available.

Fig. 3(a) shows the salinity distribution in the Chimbay area.

Fig. 3(b) shows the salinity distribution in the Kungrad area.

Fig. 4(a) shows the soil texture distribution in the Chimbay area.

Fig. 4(b) shows the soil texture distribution in the Kungrad area.

Fig. 5(a) shows the soil type distribution in the Chimbay area.

Fig. 5(b) shows the soil type distribution in the Kungrad area.

Fig. 6(a) shows the hydromorphism distribution in the Chimbay area.

Fig. 6(b) shows the hydromorphism distribution in the Kungrad area.

Fig. 7(a) shows the land management type distribution in the Chimbay area.

Fig. 7(b) shows the land management type distribution in the Kungrad area.

Figure 1

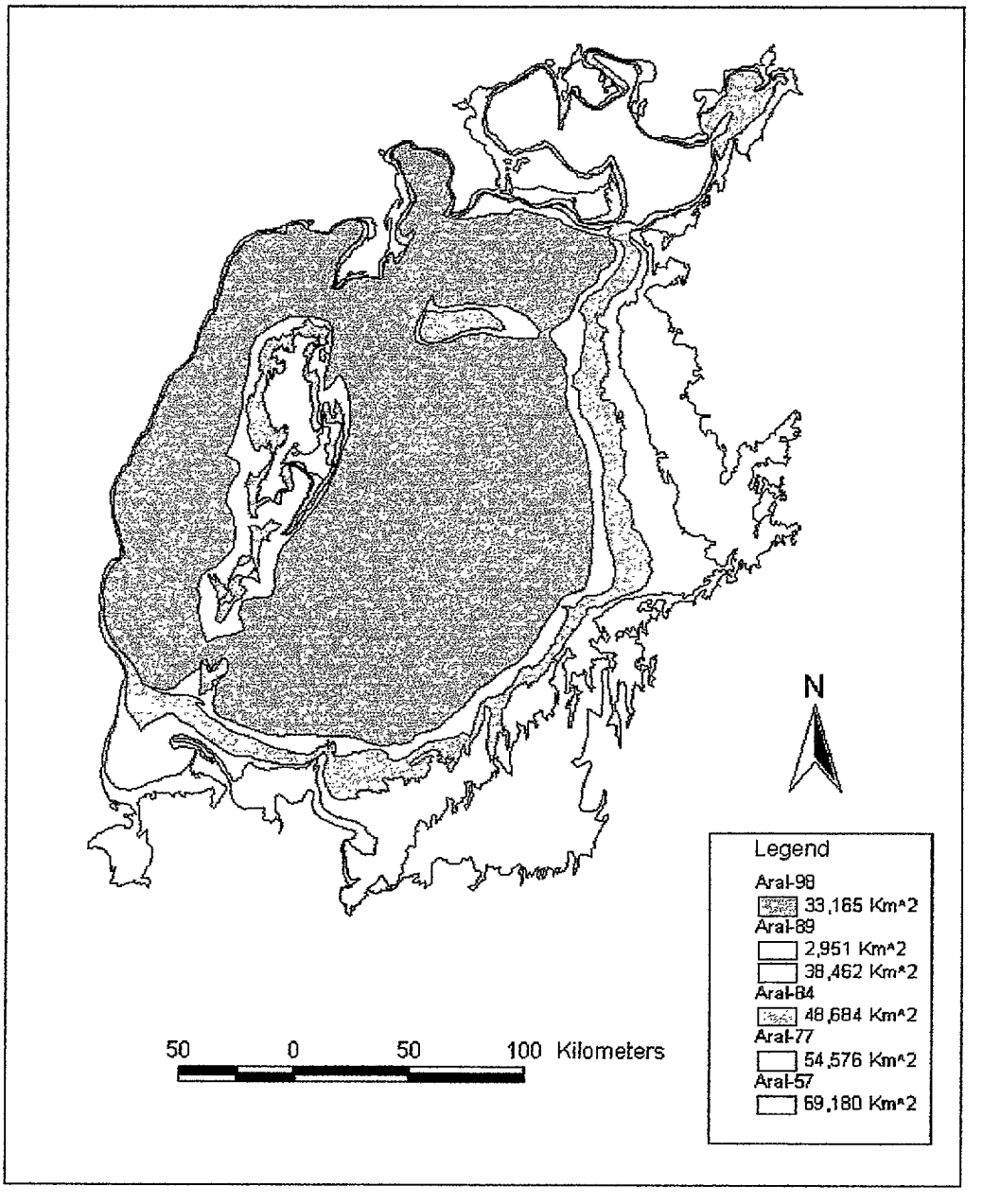
N
Legend
Aral-98
33,165 Km^2
Aral-89
2,951 Km^2
38,462 Km^2
Aral-84
48,684 Km^2
Aral-77
54,576 Km^2
Aral-57
69,180 Km^2
50
0
50
100 Kilometers

Figure 2

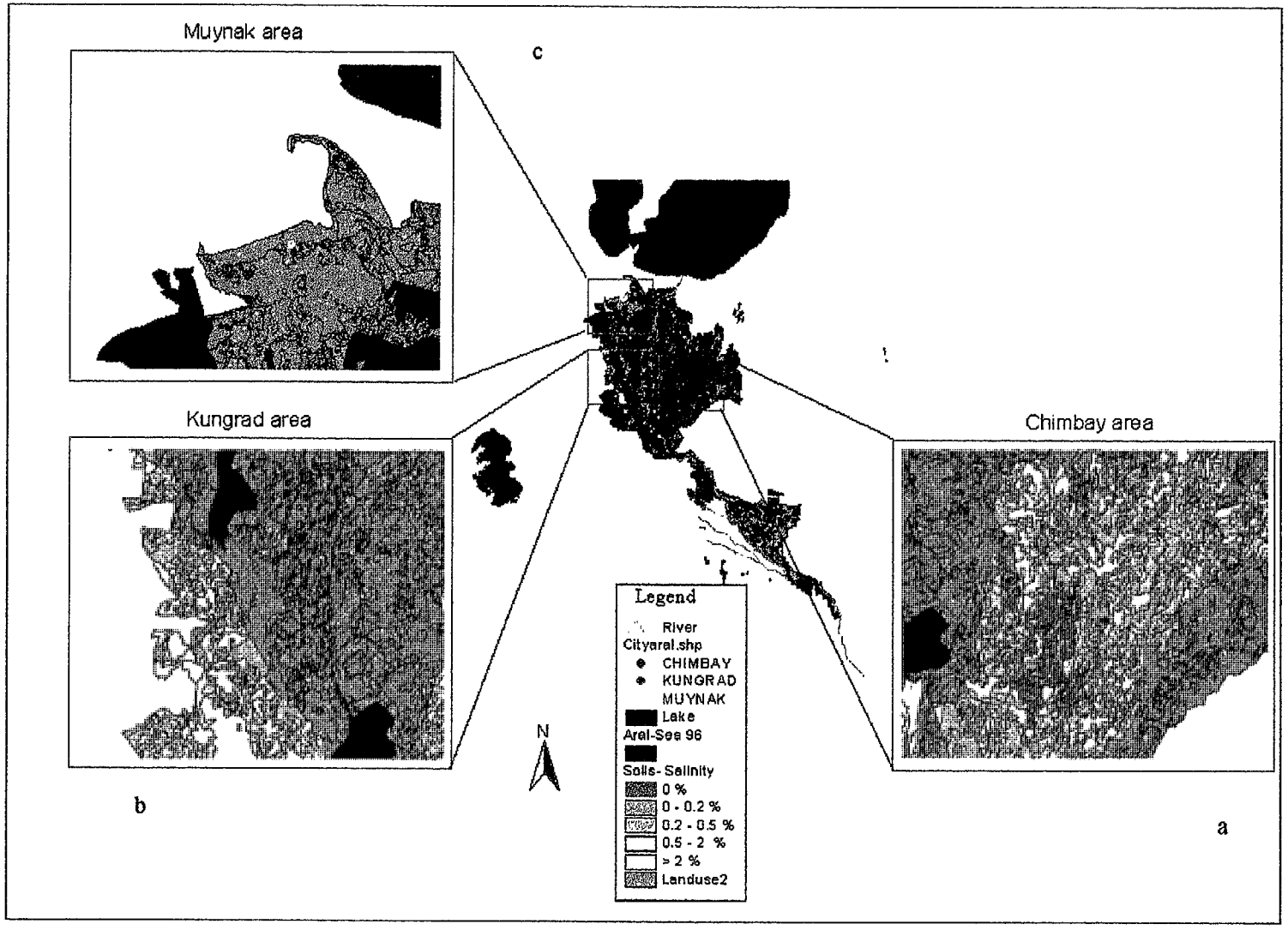
Muynak area
c
Kungrad area
Chimbay area
b
a
N
Legend
River
Cityaral.shp
CHIMBAY
KUNGRAD
MUYNAK
Lake
Aral-Sea 96
Soils- Salinity
0 %
0 - 0.2 %
0.2 - 0.5 %
0.5 - 2 %
> 2 %
Landuse2

Figure 3a

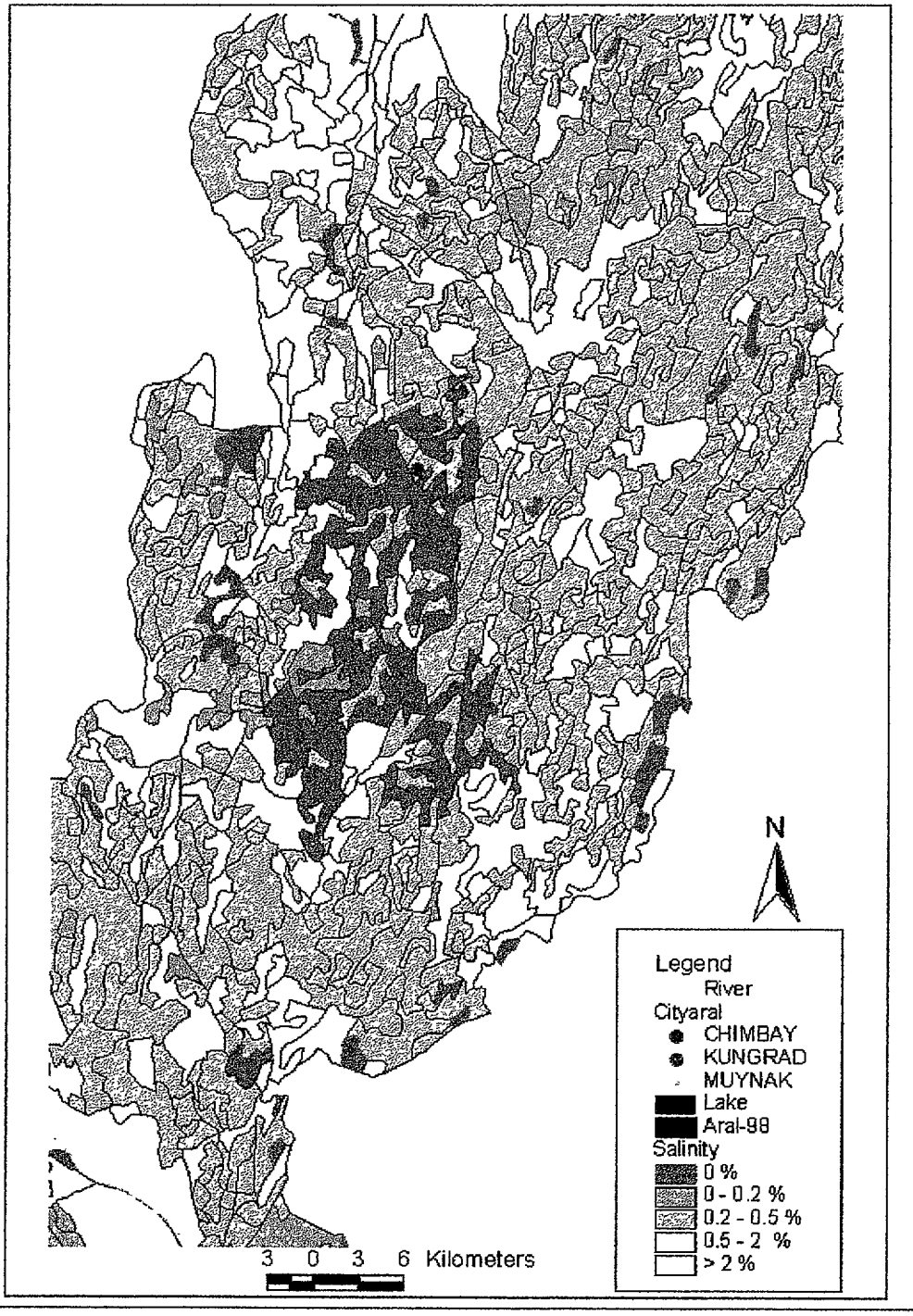
N
Legend
River
Cityaral
CHIMBAY
KUNGRAD
MUYNAK
Lake
Aral-98
Salinity
0 %
0 - 0.2 %
0.2 - 0.5 %
0.5 - 2 %
> 2 %
3 0 3 6 Kilometers

Figure 3b

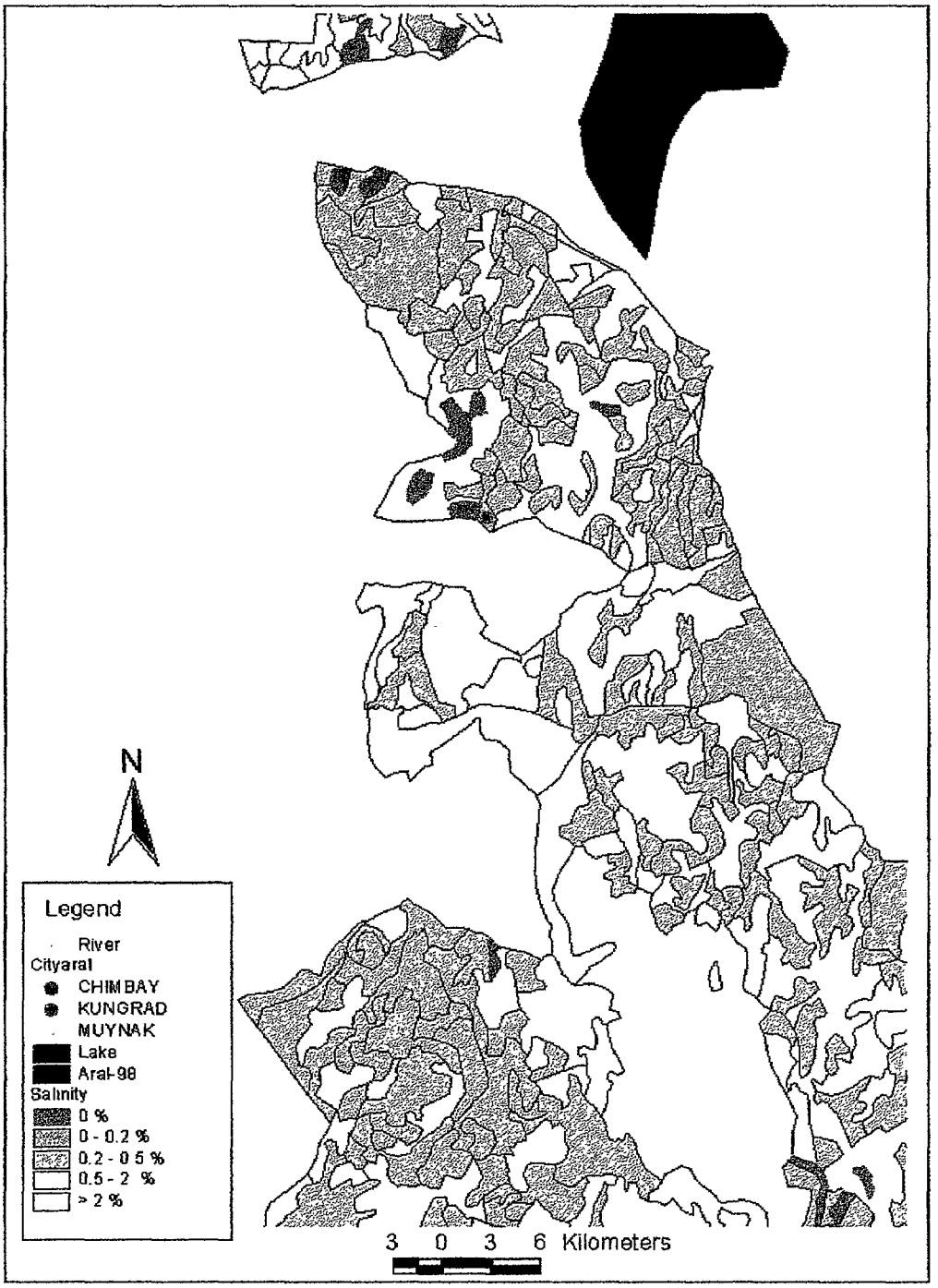
N
Legend
River
Cityaral
CHIMBAY
KUNGRAD
MUYNAK
Lake
Aral-98
Salinity
0 %
0 - 0.2 %
0.2 - 0 5 %
0.5 - 2 %
> 2 %
3 0 3 6 Kilometers

Figure 4a

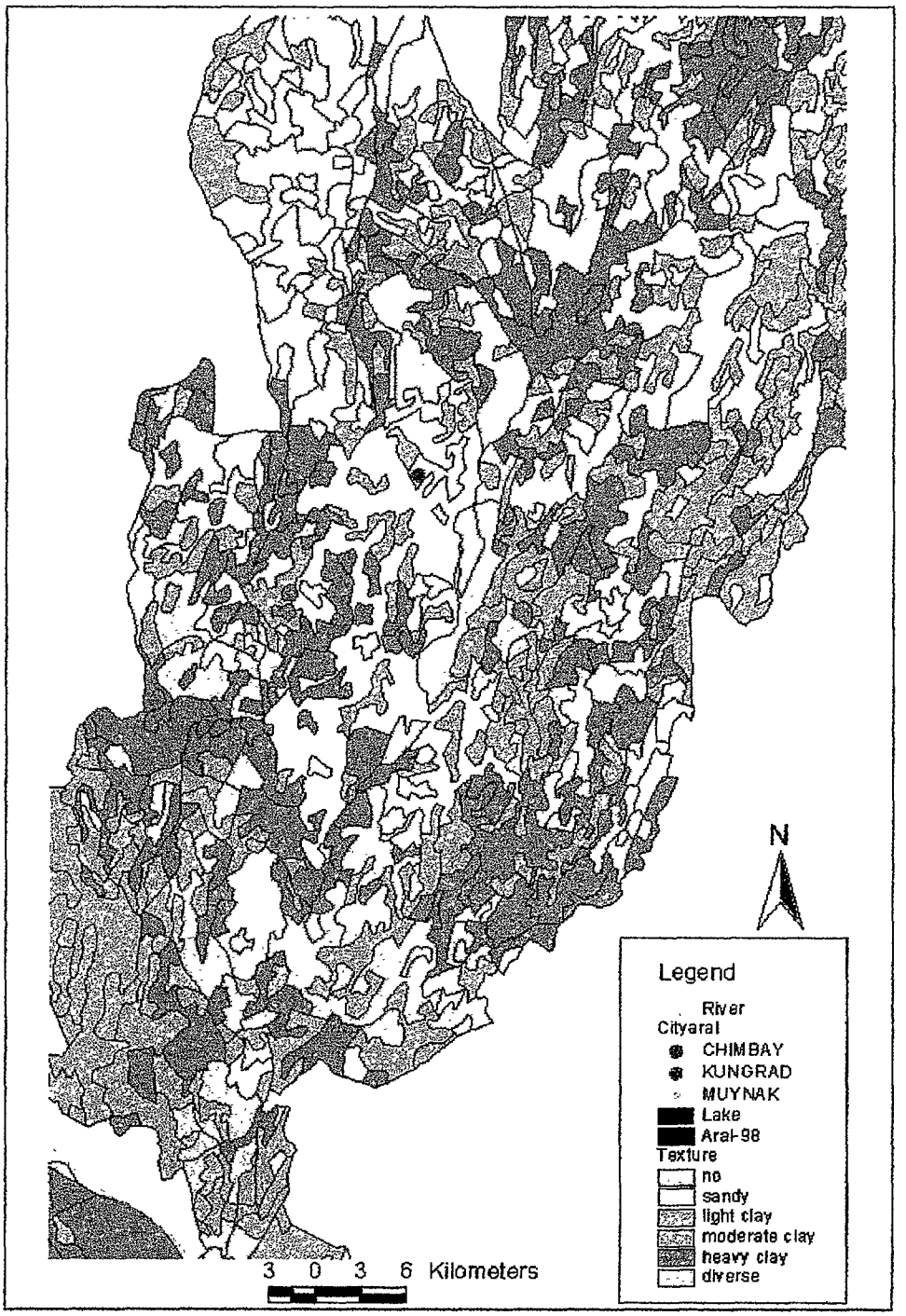
N
Legend
River
Cityaral
CHIMBAY
KUNGRAD
MUYNAK
Lake
Aral-98
Texture
no
sandy
light clay
moderate clay
heavy clay
diverse
3 0 3 6 Kilometers

Figure 4b

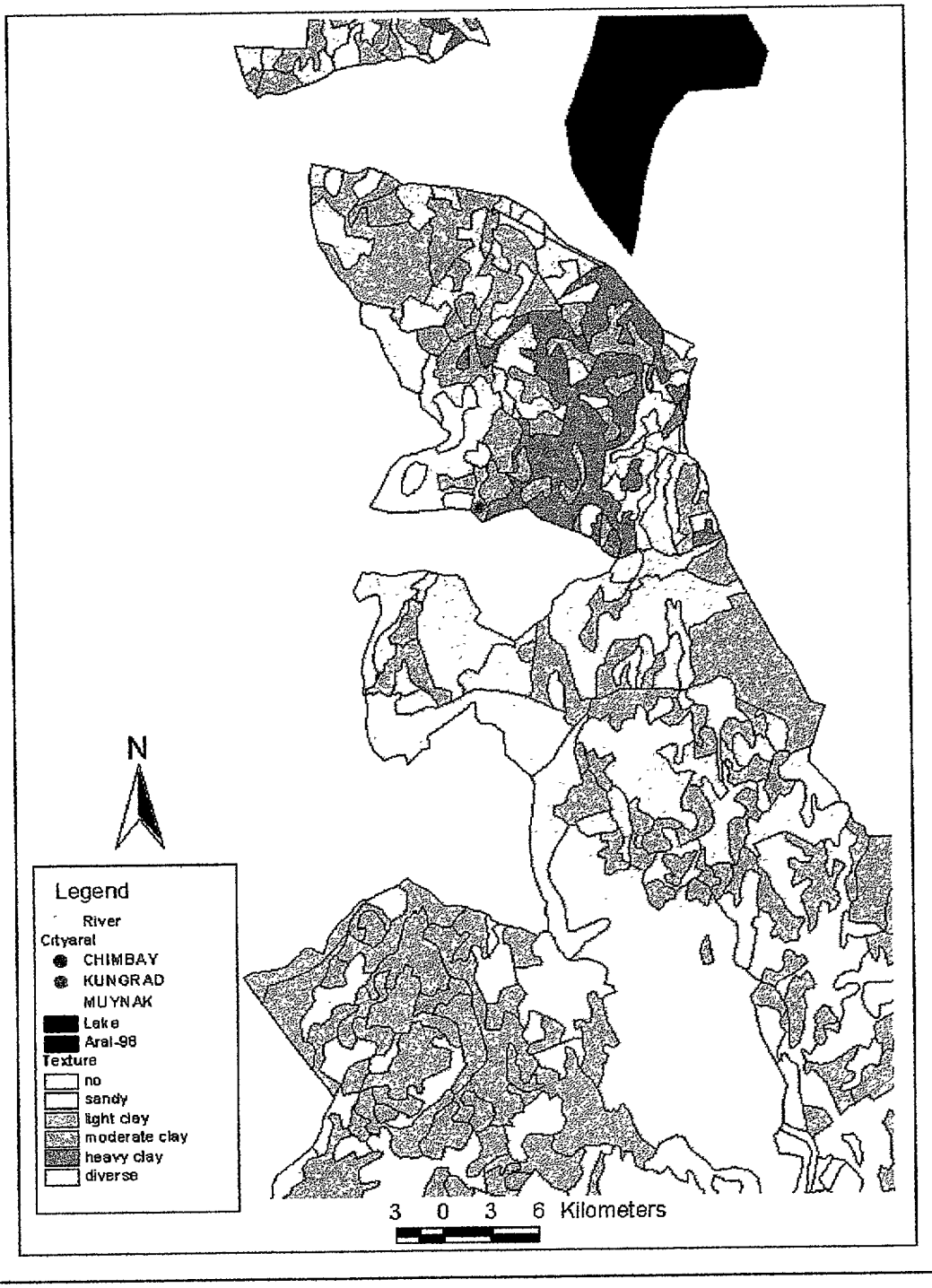
N
Legend
River
Cityarel
CHIMBAY
KUNGRAD
MUYNAK
Lake
Aral-98
Texture
no
sandy
light clay
moderate clay
heavy clay
diverse
3 0 3 6 Kilometers

Figure 5a

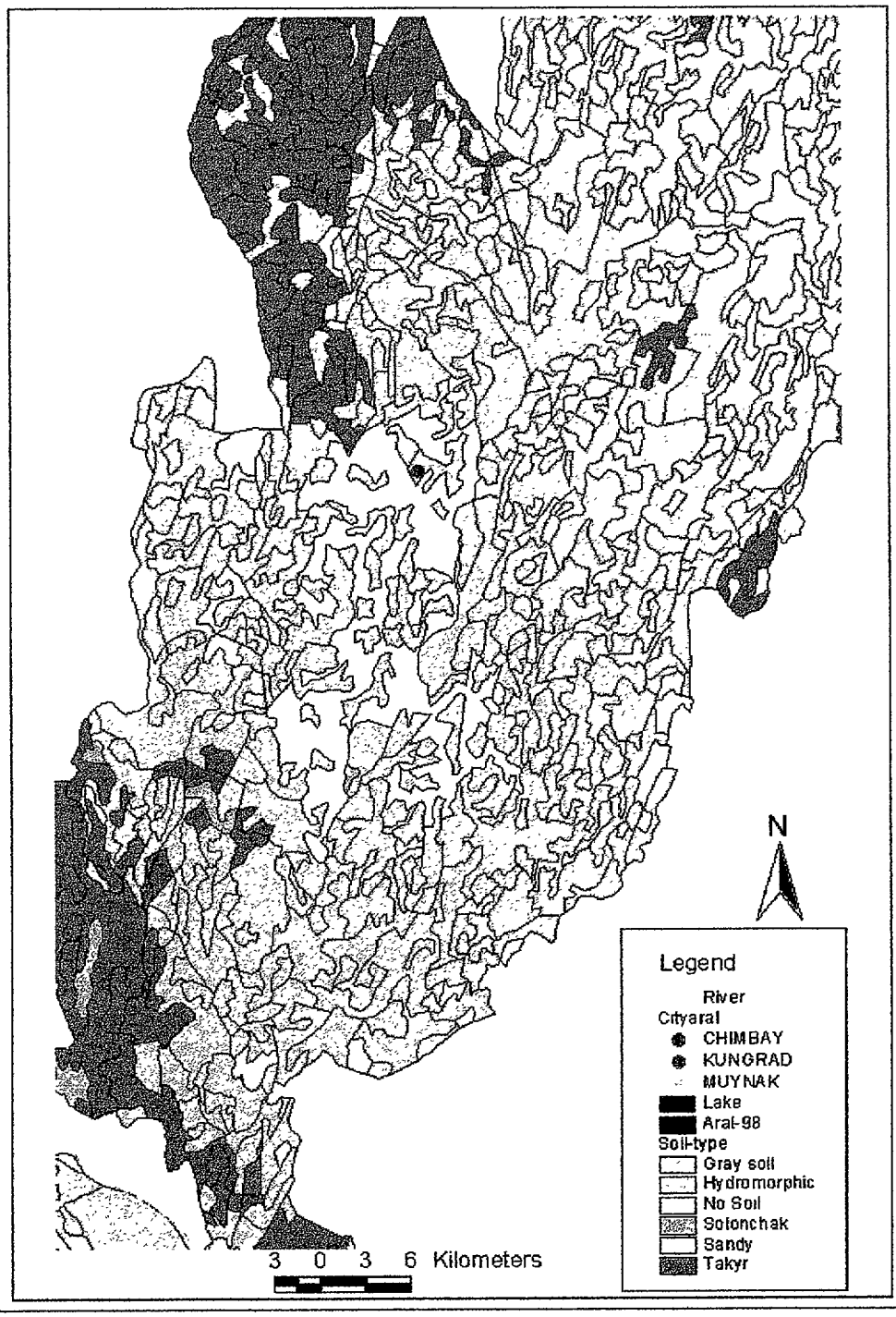
N
Legend
River
Cityaral
CHIMBAY
KUNGRAD
MUYNAK
Lake
Aral-98
Soil-type
Gray soil
Hydromorphic
No Soil
Solonchak
Sandy
Takyr
3 0 3 6 Kilometers

Figure 5b

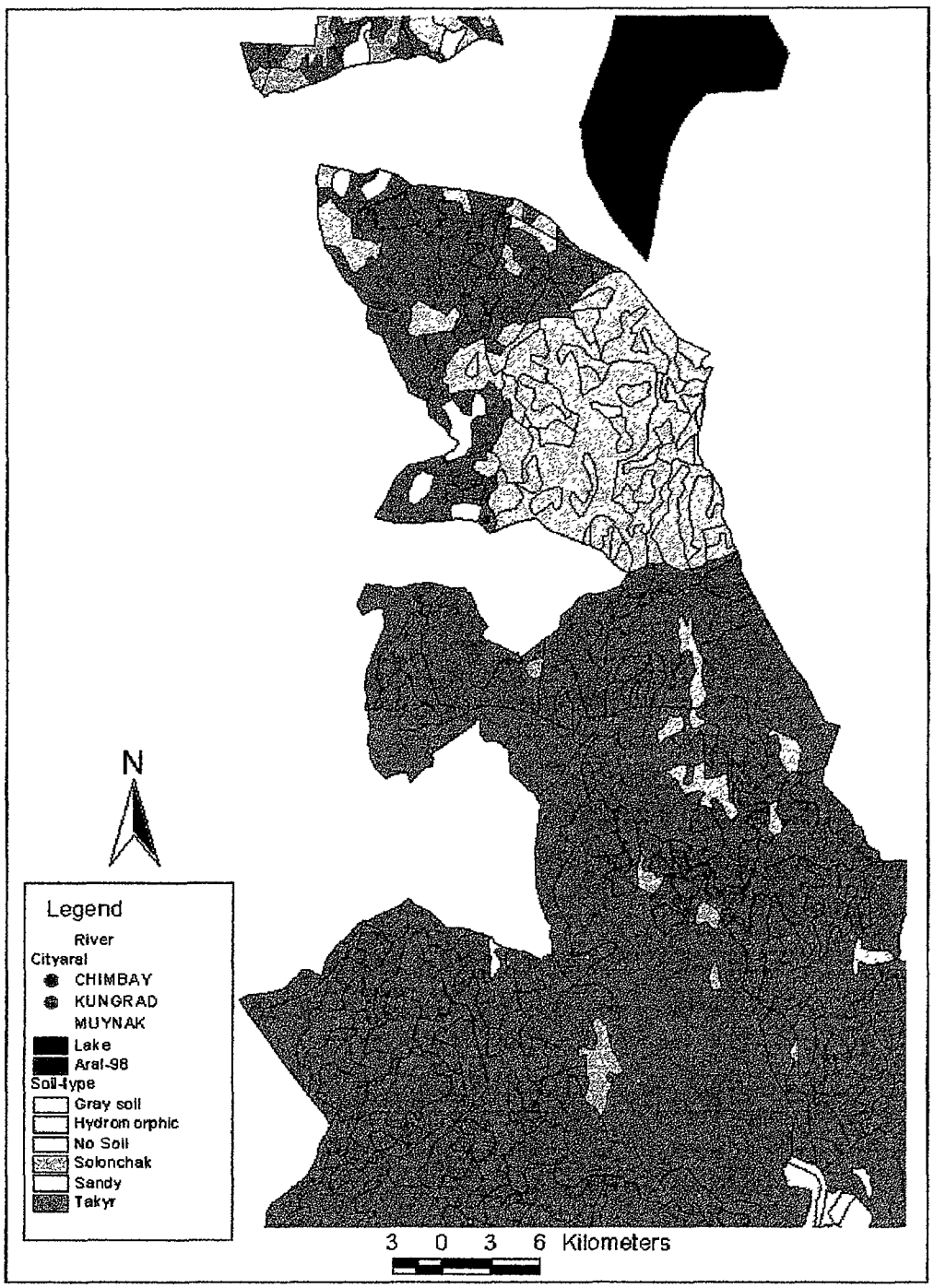
N
Legend
River
Cityaral
CHIMBAY
KUNGRAD
MUYNAK
Lake
Aral-98
Soil-type
Gray soil
Hydrom orphic
No Soil
Solonchak
Sandy
Takyr
3 0 3 6 Kilometers

Figure 6a

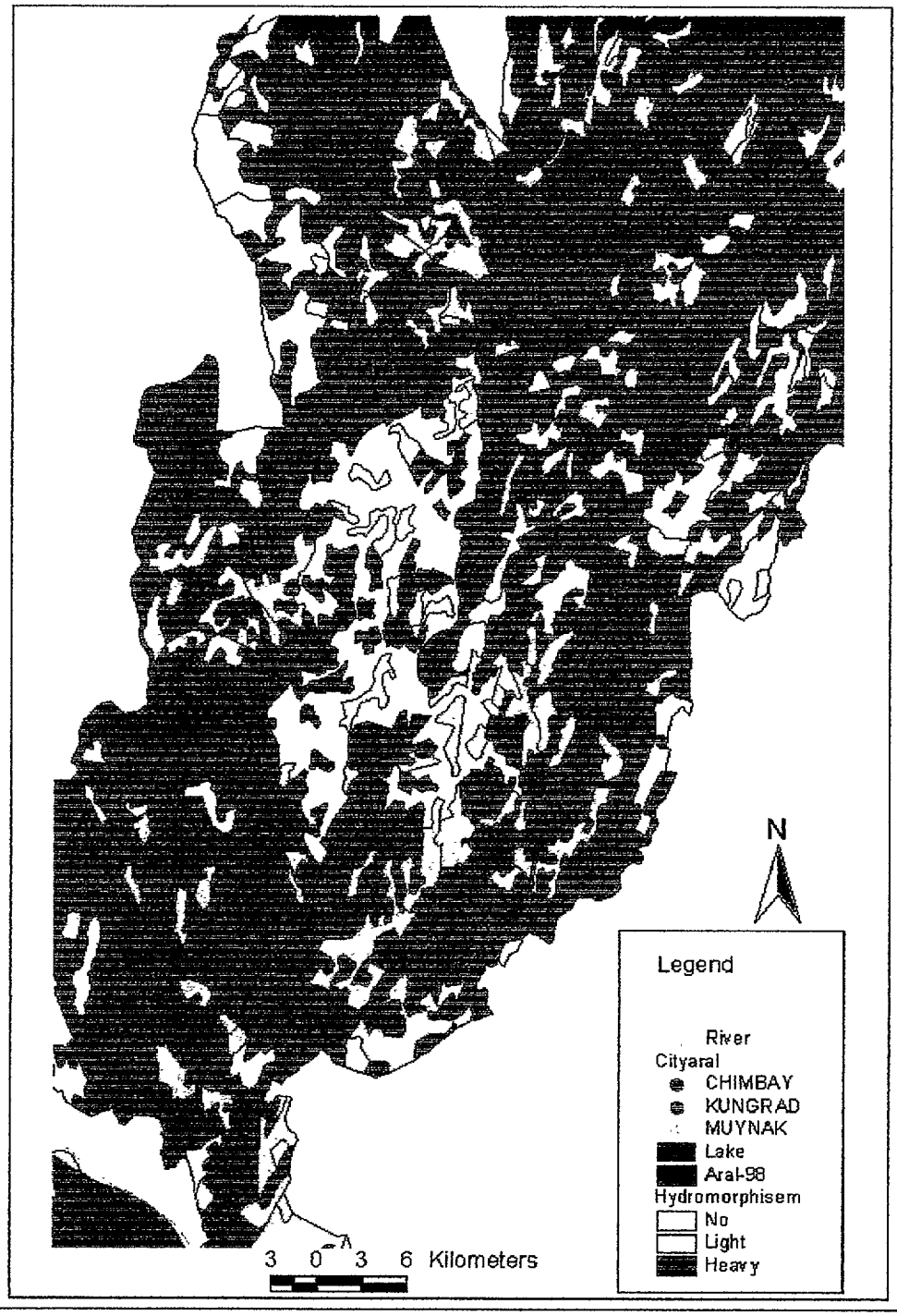
N
Legend
River
Cityaral
CHIMBAY
KUNGRAD
MUYNAK
Lake
Aral-98
Hydromorphisem
No
Light
Heavy
3 0 3 6 Kilometers

Figure 6b

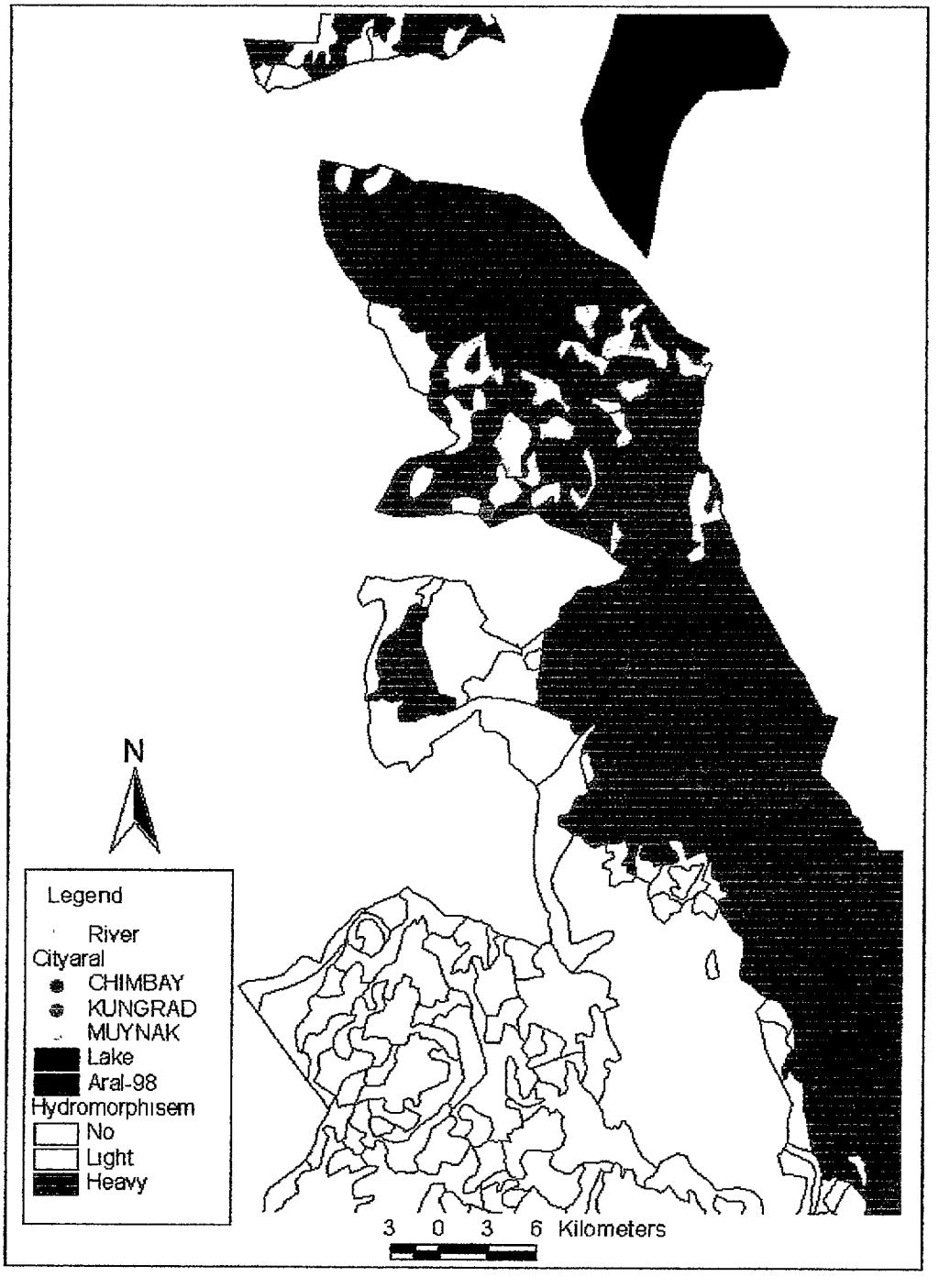
N
Legend
River
Cityaral
CHIMBAY
KUNGRAD
MUYNAK
Lake
Aral-98
Hydromorphisem
No
Light
Heavy
3 0 3 6 Kilometers

Figure 7a

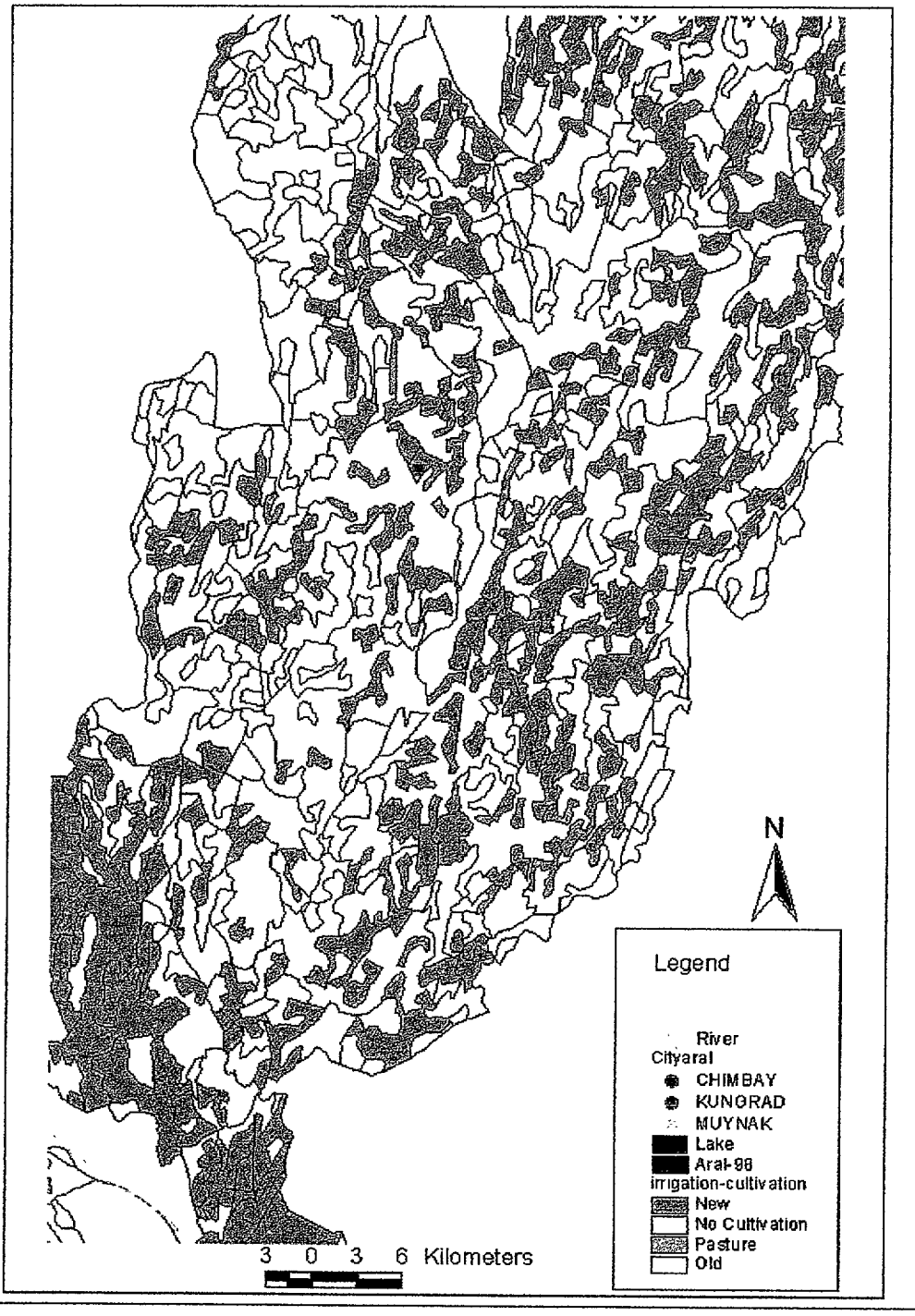
N
Legend
River
Cityaral
CHIMBAY
KUNGRAD
MUYNAK
Lake
Aral-98
irrigation-cultivation
New
No Cultivation
Pasture
Old
3 0 3 6 Kilometers

Figure 7b

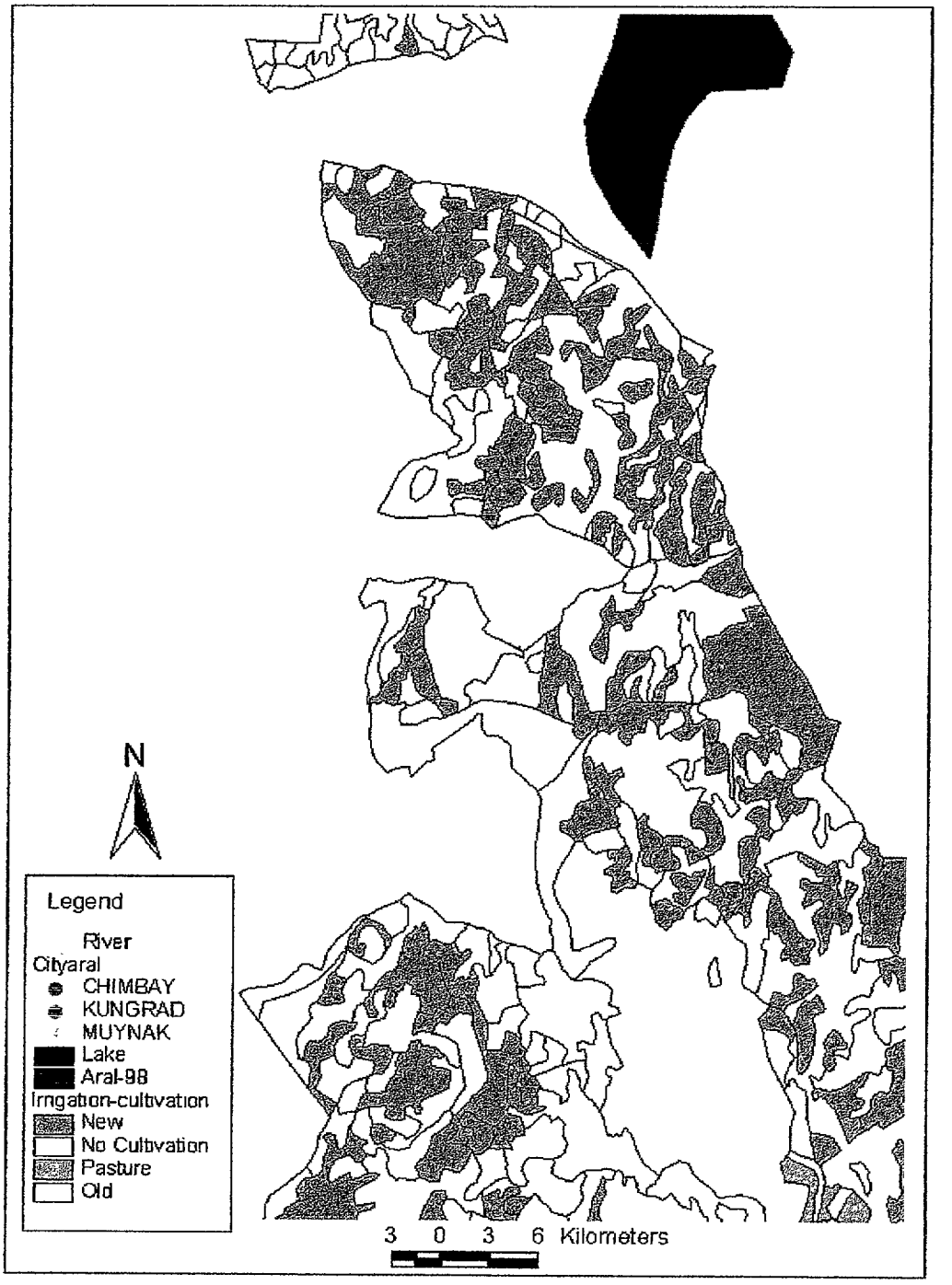
N
Legend
River
Cityaral
CHIMBAY
KUNGRAD
MUYNAK
Lake
Aral-98
Irrigation-cultivation
New
No Cultivation
Pasture
Old
3 0 3 6 Kilometers

(2) Meteorological model for dust transfer and deposition

Research Objectives

To provide recommendations related to plans for the construction of artificial water bodies/reservoirs and predict their eventual effects on the process of dust transfer/decomposition, using a numerical model.

General

Prof. Y. Mahrer participated in the international workshop on "Mineral Dust" held in Boulder, Colorado, during June 1999, and presented a paper on the application of a three-dimensional numerical meteorological model to dust generation and transport in the Aral Sea region. The paper was co-authored by E. Weinroth from Israel and M. Gilenko from Tashkent, Uzbekistan. Below is the wording of the paper.

Dust Propagation Following Desiccation of the Aral Sea

Y. Mahrer*, E. Weinroth* and M. Gilenko**

*The Hebrew University of Jerusalem, Department of Soil and Water Sciences, Rehovot 76100 Israel. **"Vodproject" Victor Malaysov Str. 3, Tashkent 7000, Uzbekistan.

A three-dimensional numerical meteorological model was used to study the process of salt transfer, propagation and deposition in the Amu Darai river delta, southern Aral Sea. Most of the dust appears to be generated by wind deflating the desiccated sea bottom, as well as adjacent areas covered with salt crusts. The dust contains up to 70% salts. These salts are distributed by the dust plume over wide distances affecting human health and contaminating soils.

The model simulates all major phases of atmospheric dust life cycles:

source and sink processes, vertical turbulent mixing, lateral diffusion and horizontal and vertical advection. One of the tasks of the model simulations was to provide recommendations related to the plans to construct artificial water bodies/reservoirs in order to reduce dust transport. In order to examine the ameliorative effect of artificial water bodies on the propagation of dust we performed three model scenarios: 1. No artificial water bodies; 2. Big artificial water bodies placed to the south of Aral Sea; 3. Small artificial water bodies to the

south of Aral Sea. The simulations were performed for two storms, one from 1991 and the other from 1993. Two dust particle sizes were considered, 2.5 m and 15 m. Results have indicated that artificial water bodies reduce the size of the dust plume.

1. Introduction

"The mighty inland Sea lies stricken now... as its waters dry to salt and blow away as noxious dust to strike the people with illness and death... " (W.S. Ellis 1990)

The atmospheric mineral dust cycle – generation, transportation, deposition and the related climatic and environmental impacts are attracting the attention of the scientific community. Long range transport of dust causes numerous environmental effects: scattering of incoming solar radiation (Carlson and Prospero, 1972; Ackerman and Chung, 1992; Chen et al, 1995; Li et al, 1996) and blooming of algae in the sea (Donaghay et al, 1992).

The local and regional transport and deposition of dust significantly influence the quality of life. In regions with high desert dust productivity, such regional dust storms can cause loss of life and serious property damages, as occurred in Egypt in May 1997 (Nickovic et al.1997).

In addition, since salts are major components of the dust, dust storms will distribute the salt over vast areas, salinizing their soils and water bodies.

Many studies used the Eulerian type transport models to gain a detailed picture of temporal and spatial distribution of dust concentration in the atmosphere and represent all major phases of dust life cycle, from deflation to deposition.

(Westphal et al, 1987, 1988; Joussaume, 1990; Nickovic and Dobricic, 1996 and Nickovic et al 1997).

This study focuses on the dust cycle in the desiccated parts of the Aral Sea. The Aral Sea, once a 26,000 square mile body of water, has now shrunk to around 40% of its former size due to the diversion of the rivers flowing into it for agricultural purposes. The receding waters have left vast areas of sea bed exposed, covered with dust composed of 70% salt. The dust has caused various health problems in the local population (Goren, 1997). This study discusses the eventual effects of constructing artificial water bodies/reservoirs on the process of dust plume transfer/deposition, and the possibility of reduction of the dust plume.

2. The model

The ETA model (Mesinger 1977,1984; Mesinger et al 1988; Nickovic et al, 1997; Janjic 1984, 1990, 1994) is used in order to calculate the dust concentration continuity equation considering the atmospheric conditions.

The model simulates all major phases of an atmospheric dust life cycle: source and sink processes, vertical turbulent mixing, lateral diffusion and horizontal and vertical advection. In the model, dust is considered as a chemically and thermodynamically passive substance of uniform particle size.

An Euler - type dust concentration equation is introduced as an additional component into the ETA coordinate model. The ETA model is a limited-area grid point model that uses the ETA vertical coordinate and includes sophisticated dynamical and physical schemes (Mesinger et al., 1988; Janjic, 1990, 1994). The ETA coordinate is a generalized sigma (mass-type) coordinate that creates step-like model mountains (Mesinger et al., 1988).

The meteorological fields are governed by aerosol-induced meteorological effects. We use a single concentration equation, assuming that the dust material contains particles of uniform size.

The dust concentration C satisfies a continuity equation of the form:

$$\frac{\partial C}{\partial t} = -u\frac{\partial C}{\partial x} - v\frac{\partial C}{\partial y} - \dot{\eta}\frac{\partial C}{\partial \eta} - \nabla K_L \nabla C - \frac{\partial}{\partial \eta}(K_H \frac{\partial C}{\partial \eta}) + S$$

Where u, v, and η are the wind components, K_H is the turbulent exchange coefficient for dust, K_L is the lateral diffusion coefficient, ∇ is the horizontal nabla operator, S is the net dust source/sink (S includes kinematic deflation of dust from the ground, wet removal by the model precipitation, and turbulent and gravitational dry deposition), and subscripts t, x, y and η denote time and space local derivatives.

Dust source areas are introduced in the Jarmoi area that was dried out. It is assumed that the process of aerosol input into the atmosphere occurs in two phases (Dobricic 1996):

1. Dust is mobilized at the ground when the lowest model level wind overcomes a threshold value.
2. The mobilized dust at the ground is vertically mixed by turbulence, as done for the other model variables.

3. Dust storm simulation

Numerical Aspects.

For the purpose of this study we chose horizontal grid interval of 0.0625 degree (16 arc min) resolution. In the vertical dimension, the atmosphere was divided into 32 layers up to the height of 17 km. The time step of the integration was 15 seconds. The model domain includes the area from latitude 37N to 52N and from 53E to 67E (the Aral Sea is at the approximate center of the domain). The large scale atmospheric conditions are inserted at the initial time and updated every six hours henceforth. The atmospheric conditions for the simulation periods were obtained from European Center Meteorological Weather Forecast (ECMWF) data. We used the 0.5x0.5 degree latitude-longitude analysis fields at standard pressure levels.

In order to check the effect of introducing artificial water bodies in the south of Aral Sea area, the numerical simulations were performed for:

1. No artificial water bodies added (PLA) (fig 1a).
2. Big artificial water bodies (BWB) added – "The big option"(fig 1b).
3. Small artificial water bodies (SWB) added - "The small option"(fig 1c).

The shapes of the proposed water bodies for each scenario were digitized into the model data. Fig 1(a, b, c) shows the refined shape of Aral Sea as obtained by observers on site. As can be seen in fig 2 the major dust sources with which we were concerned were from the dried parts of the Aral Sea.

Results

Twelve model simulations were performed for the Aral Sea area, for two storms: one on the 8-10/07/91 and the other on the 7-8/05/93.

We simulated the three above described scenarios for each storm, and for each scenario we performed one simulation with 2.5μm dust particles and another with 15 μm particles.

The difference between the BWB and SWB and PLA scenarios, is shown in figs 1(a, b, c).

The effect of the two storms on 2.5μm particle size:

The first three simulations (BWB, SWB, PLA) were performed on the storm of July 8-10, 1991. At the beginning of the storm there were north to northwesterly winds up to 10 m/s strong prevailing in the Aral Sea area.

Fig. 3(a, b, c) illustrates the calculated accumulated dust concentration near the surface during the first 30 hours (06:00- 9/7/91) of the simulation. The strong wind speed (indicated by the small arrows) caused an uptake of large amounts of dust from the surface. Values of 500 to1500 kg/km^2 can be seen in the south eastern part of the Sea. Six hundred kilometers farther to the south there is a large area of the dust cloud with a concentration of 500 kg/km^2.

In the second simulation with the small artificial water bodies (SWB) the winds that were prevailing were almost the same as in the first simulation. As can be seen in Fig. 3b, the area of dust cloud is bigger at the west and south parts of the dust clouds, than it is in the simulation of the BWB in 2% - 5% (marked by arrows). In the PLA simulation of that storm (fig 3c), we can see that there are larger areas of dust clouds than compared with the SWB simulation, as can be seen in the western part of the northern dust cloud (marked by blue arrows) and in the southern dust cloud. There is also an increase of the dust load in the middle of the southern cloud, up to 1000 kg/km^2. The difference between SWB and PLA simulations in the areas of the dust clouds is about 10%.

Six hours later, at 12:00-9/7/91, we can see in these three simulations (Fig 4.(a, b, c)) that the wind speed has decreased below 7 m/s. The main cloud is situated in the southeast part of the Aral Sea. Concentrations of 1000 kg/km^2 can be seen in the dust cloud. In the BWB simulation (Fig. 4a) the area of the dust plume is 10% smaller than that of the SWB simulation (Fig. 4b). There is an added area to the west of the main cloud (marked by a black arrow). The difference between the PLA and SWB simulation is mostly in area of the dust plume, and not in the concentration of the dust particles. This trend of differences between the BWB, SWB and PLA scenarios continued throughout the simulations of both storms with the 2.5μm particle size.

The next simulations were performed, for the same scenarios, on 15μm particles.

Fig 5(a, b, c) illustrates the calculated accumulated dust concentration near the surface after the first 36 hours (at 12:00 9/7/91). The north to northwesterly winds that prevail in the area are still up to 7 m/s. Fig 5(a, b, c) has been magnified so as to enable the viewer to discern the details in the different scenarios. As marked in fig 5(a, b) by the arrows, one can see that the area of the dust cloud in the southwest corner of Aral Sea is 5% bigger in the PLA scenario than in the SWB scenario. Comparing figures 5(b) and 5(c), we can see that the area of the

dust cloud in the BWB scenario is about 10% smaller than that of the SWB dust cloud, and the ISO-dust concentration lines are not as dense. We can see that there is also a reduction in the concentration of the dust load inside the dust cloud located 90-100 km east of the Southwest corner of the old Aral Sea.

4. Conclusions

The effect of the simulated big artificial water bodies on the dispersion of the dust clouds that pass in their vicinity is significant.

As seen in the results, there is an approximate 5% reduction of the dust load between the PLA (placebo) and SWB (small artificial water bodies) scenarios. There is 15% reduction of dust load between PLA and BWB. This reduction was consistent throughout the simulations.

Several improvements may be made with similar studies in the future. The first is a detailed examination of the effects different scenarios for the further shrinkage of lake Aral will have on dust generation and distribution. The second would be the examination of the effects of vegetation cover on dust generation. Another improvement would be comparison of the results of the simulations against true measurements.

Acknowledgments

This research was supported under Grant No. CA16-013 U.S.-Israel Cooperation Development Research Program, Economic Growth, U.S. Agency of International Development.

References

- Ackerman S.A., and Chung H., 1992: Radiative effects of airborne dust on regional energy budgets at the top of the atmosphere. *J. Appl. Meteor.*, 31, 223-233.
- Carlson T.N., and Prospero J.N., 1972: The large-scale movement of Saharan air outbreaks over the equatorial north Atlantic. *J. Appl. Meteor.*, 11, 289-297.
- Chen S.J., Kuo Y.H., Ming W., and Ying H., 1995: The effect of dust radiative heating on low-level frontogenesis. *J. Atmos. Sci.*, 52, 1414-1420.

- Dobricic S., 1996: Atmospheric transphort of desert dust toward European seas: Model parameterization and a simulated case. *Sensitivity of North Sea, Baltic Sea and Black Sea to Antropogenic and Climatic Changes.* Ozsoy E and Mikaelyan A., Eds., Kluwer Academic.
- Donaghay P.L., Liss P.S., Duce R.A., Kester D.R., Hanson A.K., Villareal T.,
- Tindale N.W., and Gifford D.J., 1992: The role of episodic atmospheric nutrient inputs in the chemical and biological dynamics of oceanic ecosystems. *Oceanography*, 4, 62-70.
- Ellis W.S., 1990: Lies Dying. *National Geographic* February 1990, 73-92.
- Ellis W.G., and Merrill J.T., 1995: Trajectories for Saharan dust transported to Barbados using Strokes's law to describe gravitational settling. *J. Appl. Meteor.*, 34, 1716-1726.
- Goren A., et al., 1997: Respiratory conditions among children associated with community exposure to airborne particles. *Environ. Res. Forum*, 8, 483-489.
- Janjic Z.I., 1984: Non-linear advection schemes and energy cacade on semi-staggered grids. *Monthly Weather Review, 112, 1234-1245.*
- Janjic Z.I, 1990: The step-mountain coordinate: physical package. *Monthly Weather Review,* 118, 1429-1443.
- Janjic Z.I., 1994: The step-mountain ETA coordinate model: Further developments of the convection, viscous sublayer and turbulence closure schemes. *Monthly Weather Review*, 122, 927-945.
- Joussaume S., 1990: Three-dimensional simulations of the atmospheric cycle of desert dust particles using a general circulation model. *J. Geophys. Res.,* 95, 1909-1941.
- Li X., Maring H., Savoie D., Voss K., and Prospero M., 1996: Dominance of mineral dust in aerosol light-scattering in the North Atlantic trade winds. *Nature* 380, 416-419.
- Mesinger F., Janjie Z.I, Nickovic S., Gavrilov D., and Deaven D.G., 1988: The step-mountain coordinate: Model description and performance for cases of Alpine lee cyclogenesis and for a case of Appalachian redevelopment. *Mon. Wea. Rev.,* 116, 1493-1518.
- Mesinger F., 1997: Forward-backward scheme, and its use in a limited area model. *Contributions to Atmospheric Physics*, 50, 200-210.

- Mesinger F., 1984: A blocking technique for representation of mountains in atmospheric models. *Rivista di Meteorologia Aeronautica,* 44, 195-202.
- Nickovic S., and Dobricic S., 1996: A model for long-range transport of desert dust. *American Meteorological Society Monthly Weather Review*, 124, 2537-2544.
- Nickovic S., 1996: Modeling of dust process for the Saharan and Mediterranean area. *The Impact of Desert Dust Across the Mediterranean*, 15-23, Guerzoni S and Chester R., Eds., Kluwer Academic Publishers.
- Nickovic S., Kakaliagou O., Kallos G., and Jovic D., 1997: ETA dust model: Sensitivity to model resolution and desert source specification.
- Westphal D.L., Toon O.B., and Carlson T.N., 1987: A two-dimensional numerical investigation of the dynamics and micro-physics of Saharan dust storms. *J. Geophys. Res.,* 92, 3027-3049.
- Westphal D.L., 1988: A case study of mobilization and transport of Saharan dust. *J. Atmos. Sci.,* 45, 2145-2175.

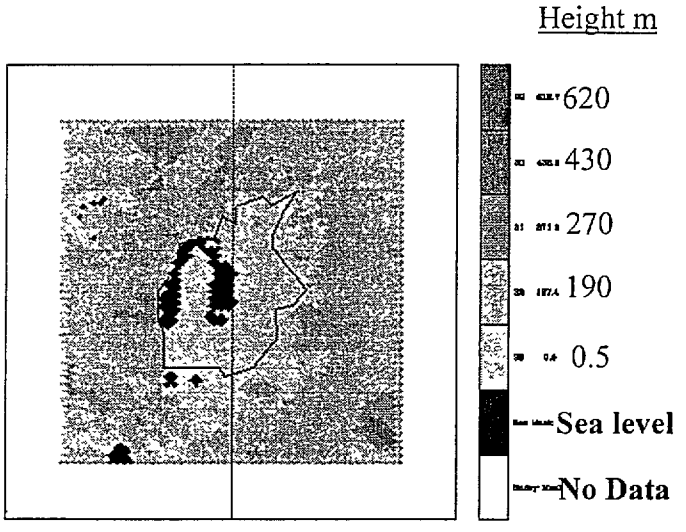

FIG 1a. The Aral Sea with no artificial water bodies

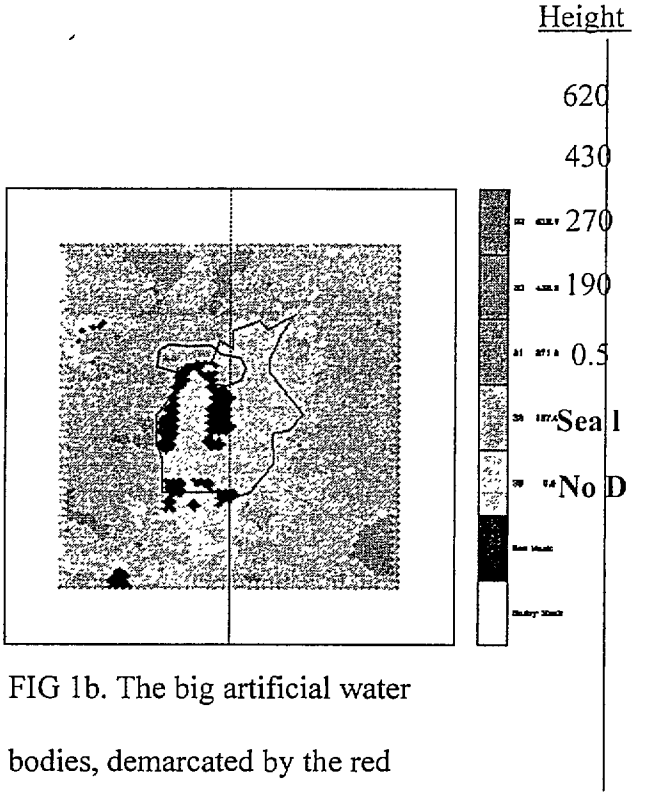

FIG 1b. The big artificial water bodies, demarcated by the red

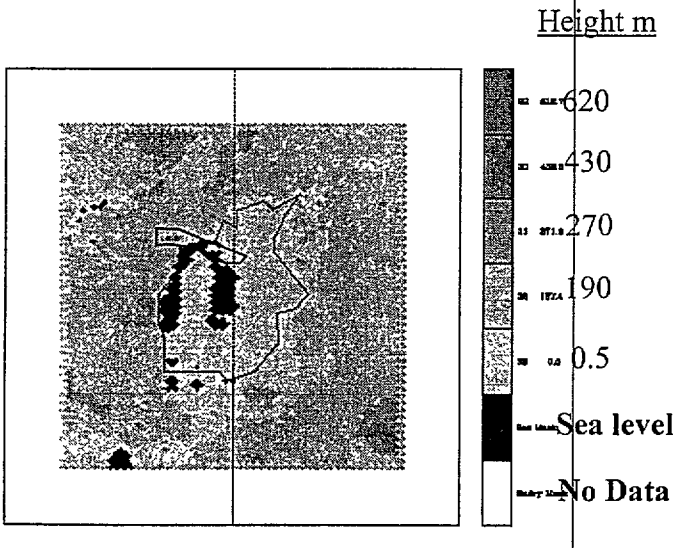

FIG 1c. The small artificial water bodies, demarcated by the yellow and black line

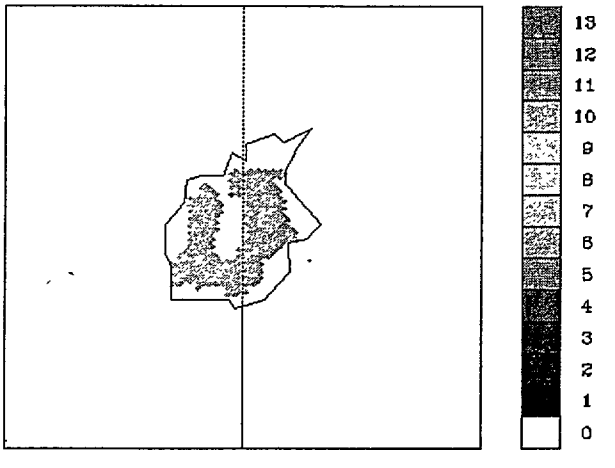

FIG 2. Dust sources from the dried areas of the Aral Sea

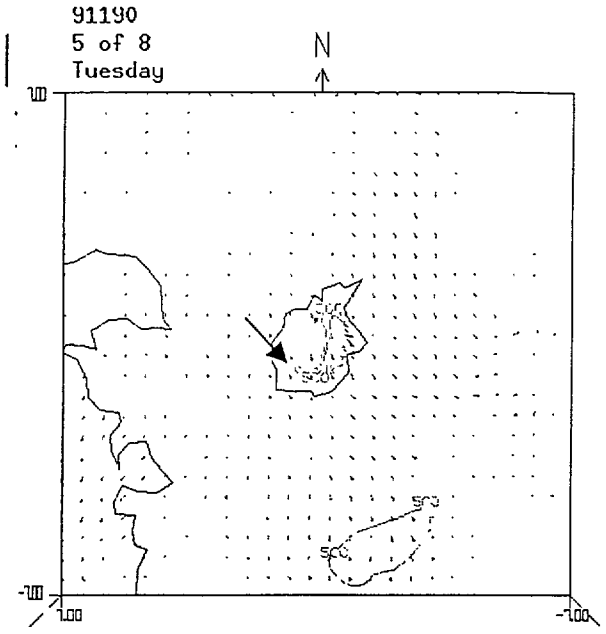

FIG 3a.

Vis5D

FIG 3a. Result of the BWB simulation. Surface Horizontal wind field and dust concentration 30 hours (06:00- 9/7/91) after beginning of the simulation. The red lines are ISO-Dust contours of dust concentration of 500 kg/km^2. Size of particles is 2.5μm.

FIG 3b. Result of the SWB simulation. Surface Horizontal wind field and dust concentration 30 hours (06:00- 9/7/91) after beginning of the simulation. Dust concentration gets to 1500 kg/km^2 in some places. The arrows mark the area with difference between the simulations.

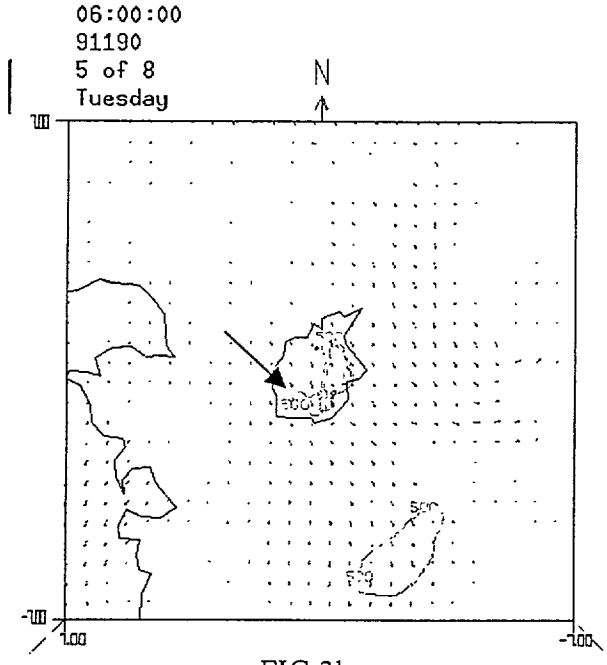

FIG 3b

Vis5D

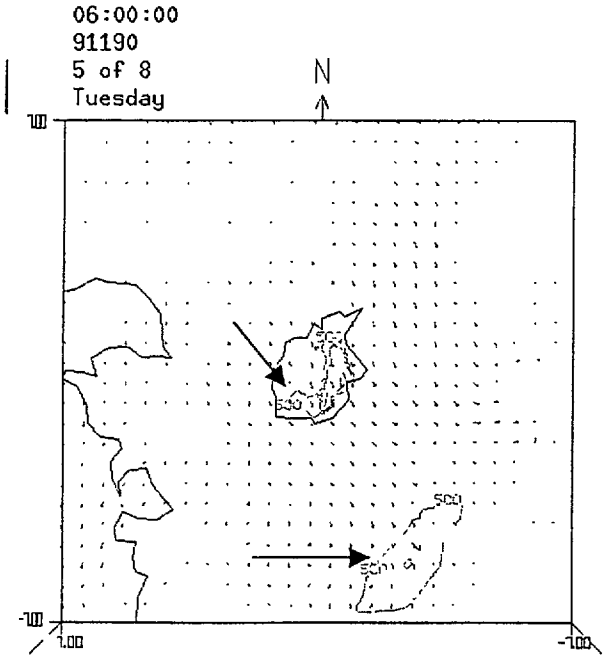

FIG 3c

Vis5D

FIG 3c. Result of the PLA simulation. Surface Horizontal wind field and dust concentration 30 hours (06:00- 9/7/91) after beginning of the simulation. Dust concentrations are about 1500 kg/km^2 in various places.

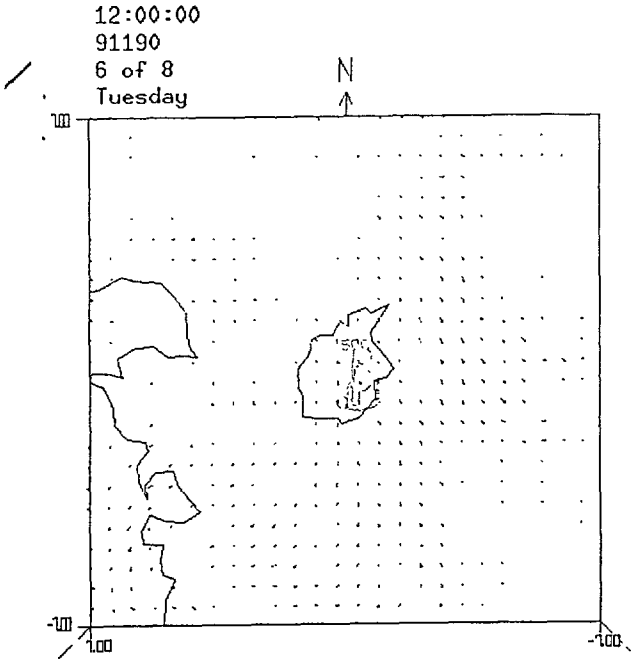

FIG 4a

Vis5D

FIG 4a. Result of the BWB simulation. Surface Horizontal wind field and dust concentration 36 hours (12:00- 9/7/91) after beginning of the simulation. The red lines are ISO-Dust contours of dust concentration of 500 kg/km^2. Size of particles is 2.5μm.

FIG 4b. Result of the SWB simulation. Surface Horizontal wind field and dust concentration 36 hours (12:00- 9/7/91) after beginning of the simulation. Dust concentrations are up to 1000 kg/km^2. The arrow marks the area of difference between the simulations.

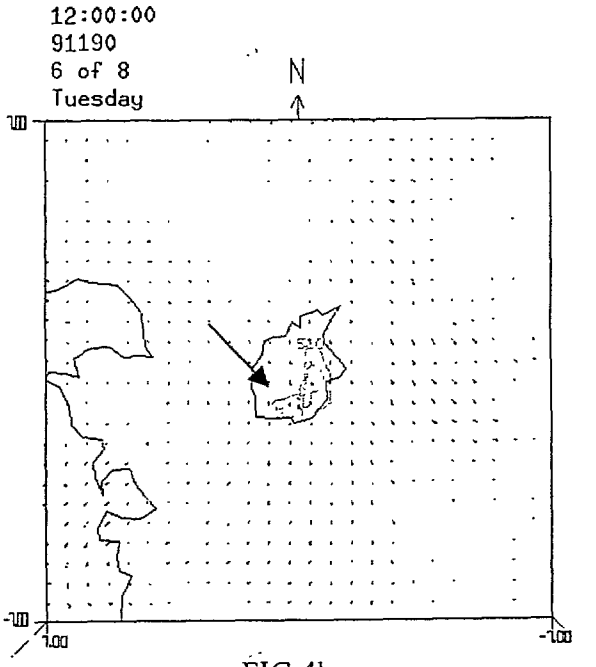

FIG 4b

Vis5

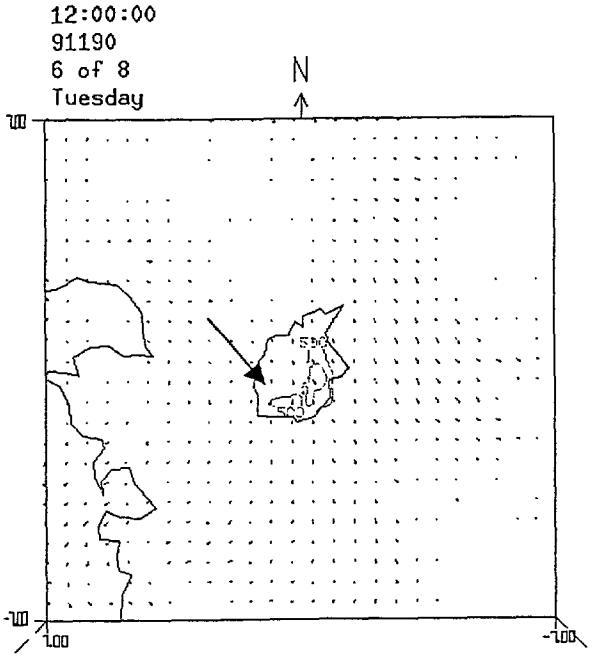

FIG 4c

Vis5D

FIG 4c. Result of the PLA simulation. Surface Horizontal wind field and dust concentration 36 hours (12:00- 9/7/91) after beginning of the simulation. The arrow marks the area of difference between the simulations.

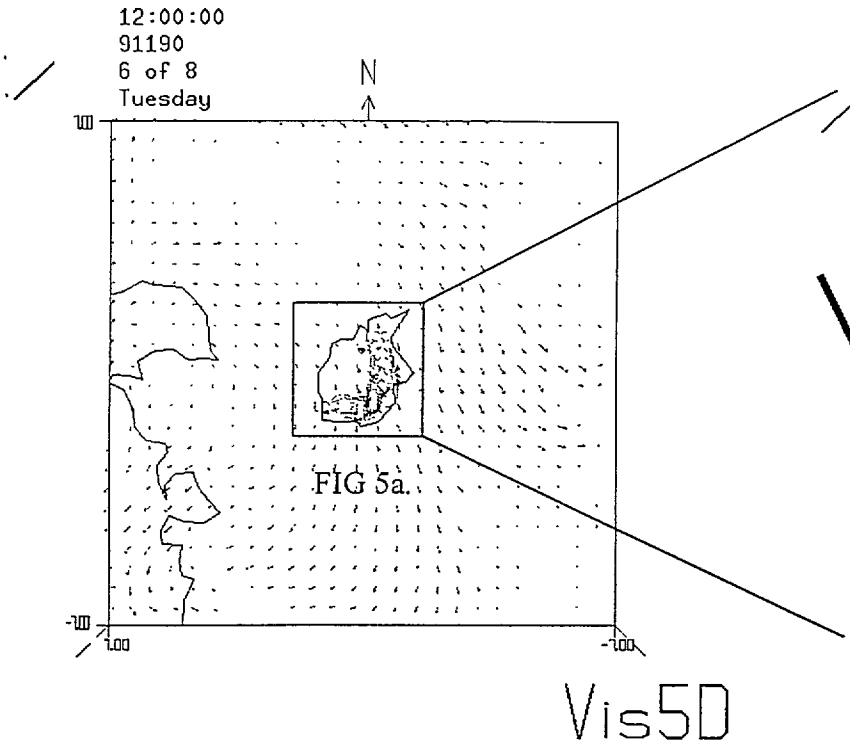

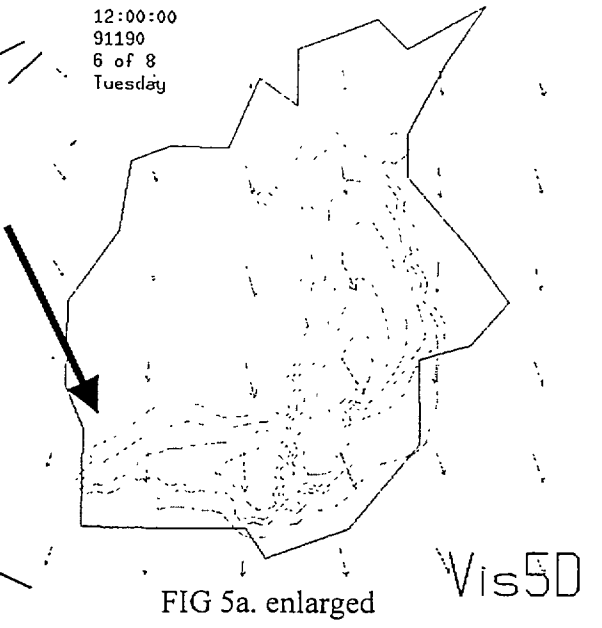

FIG 5a. enlarged

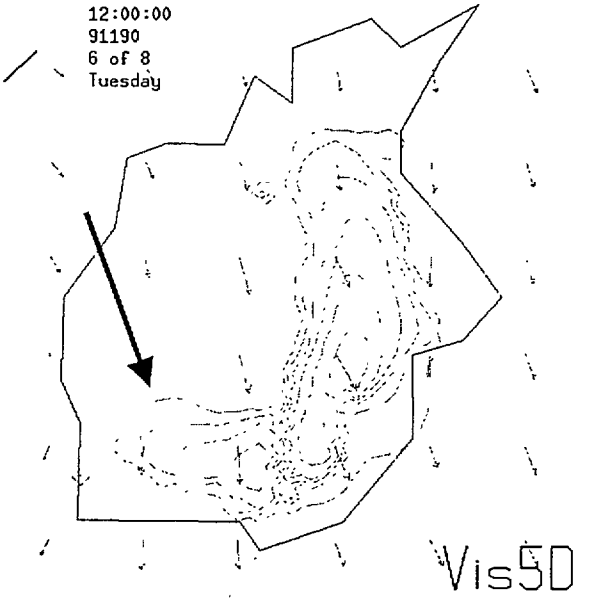

FIG 5b.

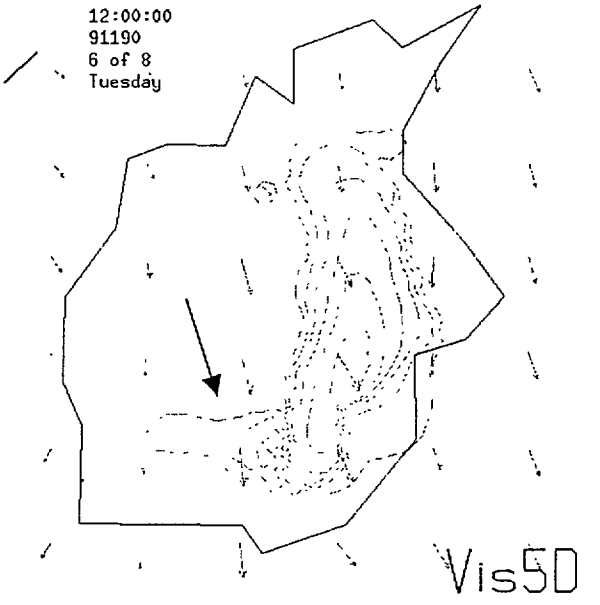

FIG 5c.

FIG 5. Surface Horizontal wind field and dust concentration 36 hr (12:00- 9/7/91) after beginning of the simulation. The red lines are ISO-Dust contours of dust concentration of 100 kg/km^2. Size of particles is 15μm.
FIG 5a. Result of the PLA simulation. FIG 5b. Result of the SWB simulation. FIG 5c. Result of the BWB simulation.The black arrows mark the area with difference between the simulations.

3) Meteorological and soil data of the Aral Sea region

Research Objectives

To provide (a) data required for dust storm modeling and for deflation studies, and (b) to provide data for an assessment of the deflation surfaces in the Amu Darai River delta.

General

For the dust storm modeling, the Uzbek partners have obtained from "Uzgidromet" updated data on wind activity in the Aral Sea region.

These wind regime characteristics are also important for the deflatability studies to be carried out in the wind tunnel in Israel. Also important for the dust storm modeling is an assessment of the soil surfaces that may serve as sources for dust entrainment. In preparation for the deflatability studies to be carried out in the wind tunnel in Israel, the Uzbek partners have prepared this study, in which the changes in moisture regime of the solonchak soils throughout the year are detailed. These soils are common in the central and northern parts of the Amu Darai River delta, and are close to the settlement of Kungrad. Industrial development is being planned for Kungrad, and therefore measures for the protection of this site from wind erosion have obtained a high degree of urgency (Figs. 1,2).

WIND CONDITIONS IN THE ARAL REGION

On the Central Asian plains, the basic factors that determine formation of conditions for wind are barometric relief and synoptic situations inherent in particular districts. These factors are substantially affected by the water area of the Aral Sea.

1. Direction of prevailing winds and their velocities

The annual wind roses are rather monotonous. Wind directions from the northeast quarter of the horizon, appropriate to the direction of barometric gradients, prevail. The mean annual wind velocities (irrespective of direction) are about 5 $m.s^{-1}$ in the western basin and about 3 $m.s^{-1}$ in the southeast region. The northern part is characterized by higher annual wind velocities (7-9 $m.s^{-1}$). On the whole, mean annual wind velocities of prevailing directions exceed the integral values. So, east winds in western parts of the region reach 6-7 $m.s^{-1}$. For the northeast part, where the winds of east and northeast directions are distributed, the mean annual velocities of 3.5-4.5 $m.s^{-1}$ are characteristic. In the southeast, weak northern and northwest winds, with velocities of 2.5-3.5 $m.s^{-1}$ are most customary.

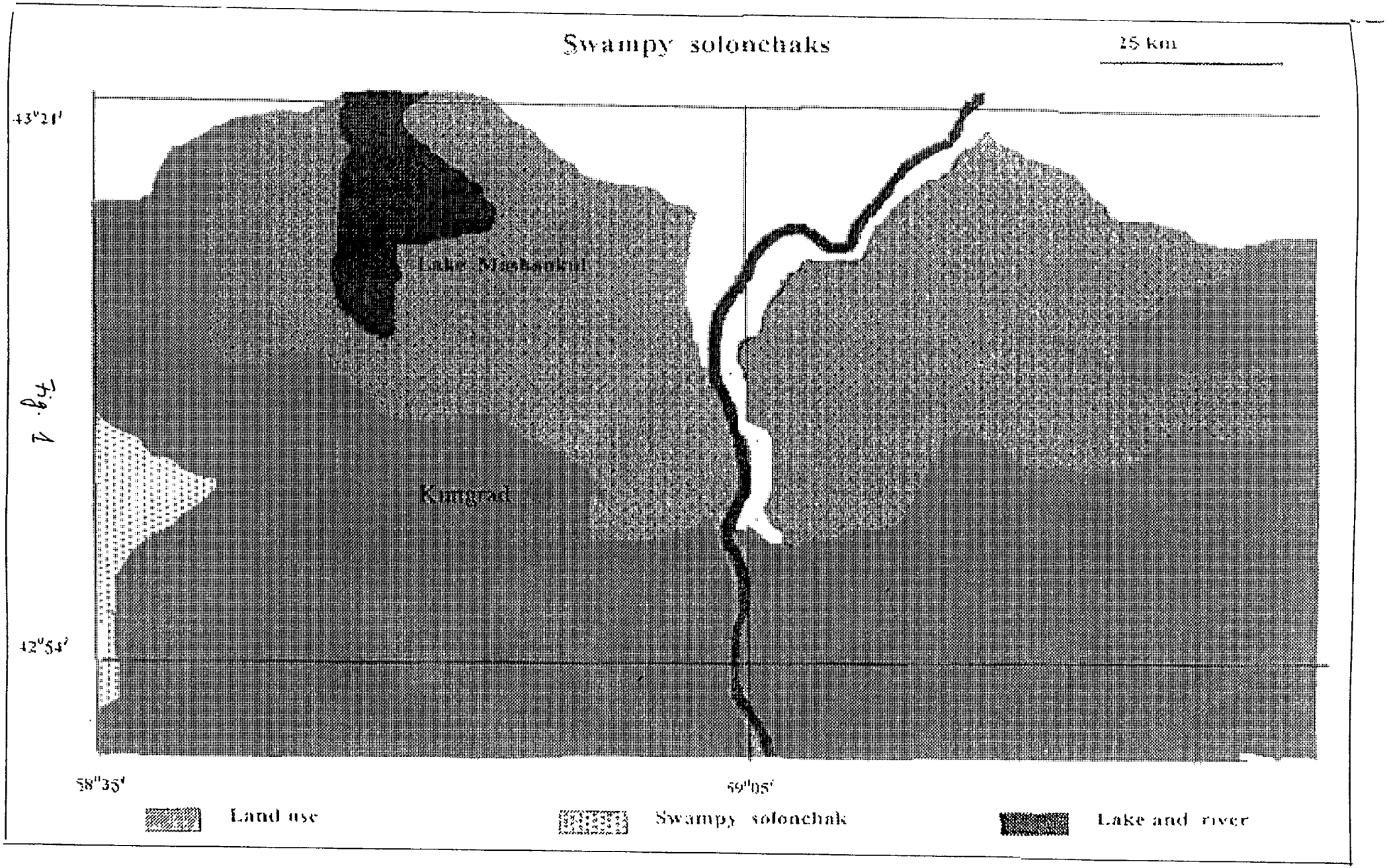
Swampy solonchaks
25 km
43°21'
42°54'
58°35'
59°05'
Lake Mashankul
Kungrad
Land use
Swampy solonchak
Lake and river

Fig. 1

The greatest mean monthly velocities of winds from east directions (6.0-6.5 $m.s^{-1}$) are observed in western parts of the investigated regions. With progress on east-northeast and east, winds weaken. Their mean monthly velocities change within the limits of 4.0-4.5 $m.s^{-1}$. north and northwest winds prevail in the south. Their monthly mean velocities do not exceed 3.0-3.5 $m.s^{-1}$.

In the spring, winds from the northeast quarter, caused by areas of raised atmospherical pressure about the territory of the Republic of Kazakhstan, prevail. Their velocities are above 4.5 $m.s^{-1}$ in the northeast part of the territory and up to 6.0-6.5 $m.s^{-1}$in the western parts.

For details of the regime data, parameters of mean annual, mean monthly, and the strong winds and their variability in time and space, the following six meteorological stations, three located in the republic of Uzbekistan and three in the Republic of Kazakhstan, are chosen:

1. Muinak, altitude of anemometer of 8 m
2. Kungrad, altitude of anemometer of 9 m
3. Nukus, altitude of anemometer of 10 m
4. Aralsk, altitude of anemometer of 10 m
5. Kazalinsk, altitude of anemometer of 9 m
6. Dzalagash, altitude of anemometer of 9m.

The materials of observation from these stations are adjusted to a uniform altitude (of anemometer) using the logarithmic law of change of velocity and direction of the wind in the surface lay atmosphere. In Table 1, the characteristics of prevailing wind directions (%) and their velocities (in $m.s^{-1}$), are presented.

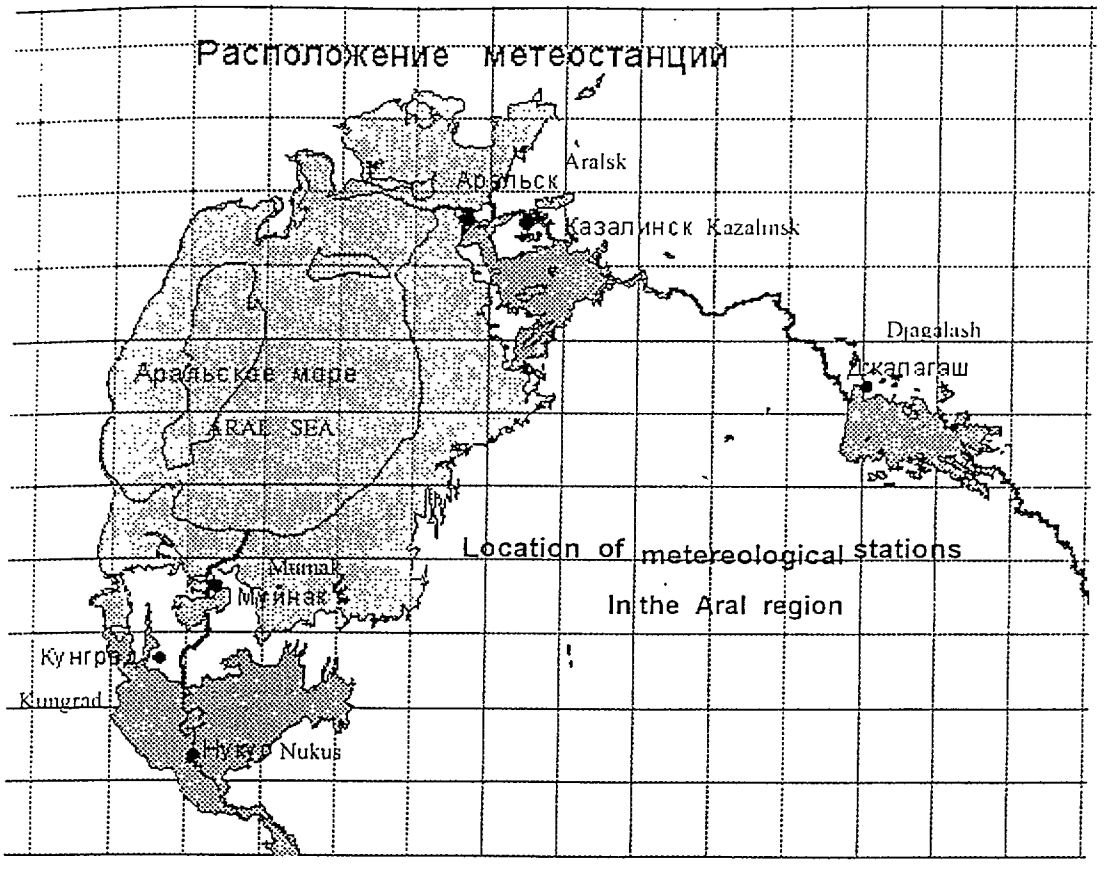

table 1. **Prevailing wind directions (%) and their mean velocities, $m.s^{-1}$.**

Station	Year			January			April			July			October		
	Direction	Frequency	Velocity	Direction	Frequency	Velocity	Direction	Frequency	Velocity	Direction	Frequency	Velocity	Direction	Frequency	Velocity
Muinak	NE N	42 38	4,2 3,9	NE N	38 36	4,0 3,9	NE	52	6,8	NE N	41 29	4,2 4,0	NE	48	4,0
Kungrad	N	53	3,8	N	40	4,1	NE N	39 42	6,1 6,0	N	41	5,8	NE	39	4,0
Nukus	NE	36	4,3	NE	36	4,5	NE	29	4,6	N NE	28 28	3,4 3,8	NE	37	3,6
Aralsk	NW	29	5,8	NW	29	4,2	NW W	38 21	7,0 5,9	NW W	28 28	4,0 3,5	NE	37	2,9
Kazalinsk	W	32	4,1	W	40	4,4	W NW	29 30	5,6 4,9	W	28	4,0	W NW	29 40	3,9 4,1
Djagalash	W	35	4,3	W	41	3,8	W	45	5,8	W	41	4,9	W	35	3,8

2. Mean wind velocities and their annual course

The mean annual wind velocity varies within the limits 3-5 $m.s^{-1}$. The eastern part of the region is characterized by weaker wind activity compared to the western part. The annual number of wind calms changes very strongly – from 22 (Muinak station) up to 157 (Nukus station). The greatest mean wind velocities on the plains of Central Asia, as well as in the investigated territory, are observed, as a rule, in spring. In the summer, secondary, weaker maxima are common. The lowest mean monthly wind velocities are usually observed in autumn or winter (Table 2).

Table 2. Mean monthly and annual wind velocity ($m.s^{-1}$) and annual number of calms

Station	I	II	III	IV	V	VI	VII	VIII	IX	X	XI	XII	Year	Number of calms
Muinak	4,9	5,1	5,4	5,6	5,1	4,3	4,0	4,2	3,8	3,6	3,8	3,9	4,5	22
Kungrad	4,8	4,9	5,0	5,1	5,0	4,1	3,8	3,9	3,9	3,8	3,9	4,0	4,3	69
Nukus	4,1	3,9	4,2	4,3	4,0	3,2	3,3	3,4	2,8	2,7	3,1	3,3	3,5	157
Aralsk	4,9	5,2	5,5	5,8	5,0	4,4	4,2	4,0	3,9	4,0	3,9	4,0	4,6	31
Kazalinsk	4,7	5,0	5,2	5,4	4,8	4,2	4,0	4,0	3,9	3,8	4,0	4,1	4,4	36
Djagalash	4,5	4,8	5,0	5,1	4,7	4,1	4,0	3,8	3,8	4,0	3,9	3,8	4,3	45

3. Strong winds

According to the classification adopted in the Republic of Uzbekistan, strong winds are those with a velocity of 15 $m.s^{-1}$ and more. Annual number of days with a strong wind differ considerably. The frequency and duration of strong winds decrease from the north to the south. So, the number of days with a strong wind is 29 in Aralsk and 20 in Muinak, and only 12 in Nukus and 11 in Dzalagash. A full representation about number of days with a strong wind and its annual distribution is given in Table 3 and Fig. 3

As can be seen, the greatest number of days with a strong wind are observed in the transition months. During the summer and winter months, some recession of wind activity takes place. Winds with the greatest velocities in the winter come from the southern direction. They arise usually as gusts of southern cyclone collectors. The strong winds from the northern direction in the winter are observed everywhere, but usually do not equal in velocity to winds from the southwest direction. In the summer, the strongest winds have a

northern direction. They arise as a result of cold intrusions from high latitudes. During the autumn months, with the renewal of cyclonic gusts, the greatest velocities of winds of a southwest direction are again marked.

Table 3. Average of days with a strong wind (means for 1982-1997).

Station	I	II	III	IV	V	VI	VII	VII	IX	X	XI	XII	Year
Muinak	0,7	1,5	2,2	2,3	2,9	1,3	0,4	0,6	1,7	2,0	3,2	0,4	20
Kungrad	0,9	1,1	1,5	1,9	1,5	2,0	0,8	0,9	0,4	1,0	0,9	0,3	13
Nukus	0,8	1,0	1,4	1,8	1,4	1,9	0,8	0,8	0,3	0,9	0,9	0,2	12
Aralsk	1,6	2,1	2,6	3,6	3,8	1,9	0,9	1,2	2,3	3,6	4,4	1,0	29
Kazalinsk	1,4	1,9	2,3	3,1	2,9	0,9	0,6	1,4	2,2	2,1	3,3	0,9	23
Djalagash	0,7	0,9	1,3	1,7	1,3	1,8	0,8	0,7	0,2	0,8	0,9	0,1	11

4. Threshold wind velocities

It is accepted to consider that deflation begins at some threshold wind velocities, sufficient for separation of soil particles from a surface. The value of threshold velocities depends on the topography of ground, its mechanical structure and moisture, density of a vegetative coverage, etc. According to some data (1), threshold velocity on an agricultural field are 3-5 $m.s^{-1}$, but can have higher values.

Unfortunately, special researches directed on an estimation of threshold wind velocities for surfaces of solonchaks or dried bottom of the Aral Sea, are lacking, though these surfaces are the greatest contributors to deflation. Not only strong, but common winds are capable of causing a dangerous level of deflation. The characteristic example is described in the special literature (2). Salts on the dried bottom of the Aral Sea are basically (60-80% of samples) – sulphates. During deposition of precipitations, the surface forms a strong crust, if the moisture is equal to field capacity. The mineral "Thenardite" forms a white powder on the surface with decrease of moisture. This powder is easily blown off even at minor (about 1 $m.s^{-1}$) winds, it forms again and is again blown off. Thus, the production of thenardite and its consumption by deflation into the atmosphere continuously works. It is important to note that thenardite is characterized by high chemical activity. Getting into human and animal breathing organs, thenardite is instantly enveloped by molecules of water, forming microscopic ulcers covering internal cavities. For this reason, the overwhelming majority of inhabitants in the Aral Sea regions are ill with tuberculosis, asthma, and bruselosis in this or

that form. On this basis, we may conclude that the characteristic parameters of a wind should include not only high, but also mean velocities.

Full-scale observations for 47 years allow to use the methods of mathematical statistics for objective definition of design parameters of wind activity. For obtaining wind velocities of required probability, it is necessary to manipulate the information using the following statistical parameters.

1. Mathematical expectation $\bar{V}=\frac{\sum_{i=1}^{n} V_i}{N}$

2. Factor of a variation $Cv(V)=\sqrt{\frac{\sum_{i=1}^{n} (K-1)^2}{n}}$

3. Factor of asymmetry $Cs\ (V) = \frac{\sum_{i=1}^{n} (V_i - V)^3}{N\ C_v^3}$

The following conventional signs are hereinafter adopted: V – mean wind velocity; N – number of the members of a statistical series; Cv(V) – factor of a variation of wind speed; K=Vi/V – modular factor of wind velocity; Cs(V) – factor of statistical series asymmetry.

Among adduced indexes, the definition of factor of asymmetry is most important. It is a dimensionless statistical parameter describing a degree of an asymmetry of a series of considered set of wind velocities concerning its mean value. The difficulty consists in necessity of the extremely large sample from general set so that the determined value, Cs, was incommensurably above its random error. Therefore, with reference to wind velocities, it is considered expedient to execute calculation Cs(V) under the formula. L. Hersman (3), who empirically takes into account incomplete samples

$$Cs(V) = 2{,}648\ CV(V) - 0.645$$

Now it is obviously possible to construct a curve of probability of wind velocities (for example in Figure 1) and to determine with its help modular parameters of mean and maximum wind velocities.

Table 4. Average (nominator) and maximum (denominator) wind velocities ($m.s^{-1}$).

Station	Frequency (%)							
	1	3	5	10	50	75	90	95
Muinak	5,8 10,4	2,6 9,8	5,1 9,6	4,9 8,9	4,5 8,1	3,9 7,3	3,7 6,0	3,1 5,7
Kungrad	5,5 8,7	5,3 8,1	5,0 7,8	4,7 7,3	4,3 6,8	4,1 6,3	3,8 5,9	3,5 5,2
Nukus	4,5 6,3	4,2 6,0	3,9 5,7	3,7 5,2	3,5 4,9	3,2 4,3	3,0 4,0	2,8 3,7
Aralsk	5,9 11,1	5,6 9,8	5,0 9,3	4,8 9,0	4,6 8,7	4,4 8,2	4,2 7,6	3,9 6,1
Kazalinsk	5,6 10,9	5,2 10,0	4,8 9,6	4,6 9,1	4,4 8,5	4,1 7,2	3,8 6,8	3,3 6,1
Djagalash	5,5 10,7	5,2 10,0	5,0 9,7	4,6 9,0	4,3 8,4	4,1 8,1	3,8 7,5	3,5 7,0

Table 4 gives the values of mean and maximum wind velocities for each month of the year. For protection of oases, settlements and other objects from harmful atmospheric depositions caused by deflation, it is necessary to know not only computed velocities of a wind, but also its most probable direction. Only in these case methods of protection, by decreasing deflation surfaces with active substances will get purposeful and subject character. From this point of view, the results of statistical definition of probability of this or that wind direction (Table 5) are of interest.

Table 5. Probability (%) of wind directions in the region of the southern Aral.

Month	N	NE	E	SE	S	SW	W	NW	Calm
January	9	30	20	8	7	6	9	11	16
February	13	33	16	7	4	7	9	11	14
March	17	26	16	8	4	5	10	14	11
April	17	28	18	7	3	6	8	12	10
May	18	31	18	6	3	4	8	13	9
June	23	32	15	4	2	3	7	14	12
July	23	31	15	5	2	3	6	15	15
August	25	36	14	3	2	2	7	11	16
September	18	32	17	5	2	3	8	15	18
October	11	24	21	8	4	5	11	16	22
November	9	30	21	8	6	5	10	11	19
December	7	32	20	8	7	7	8	11	17
Year	16	30	18	6	4	5	8	13	15

Curve of probability of mean wind speeds (with the guarantee correction)

fig.1

Кривая обеспеченности средних скоростей ветра (с гарантийной поправкой)

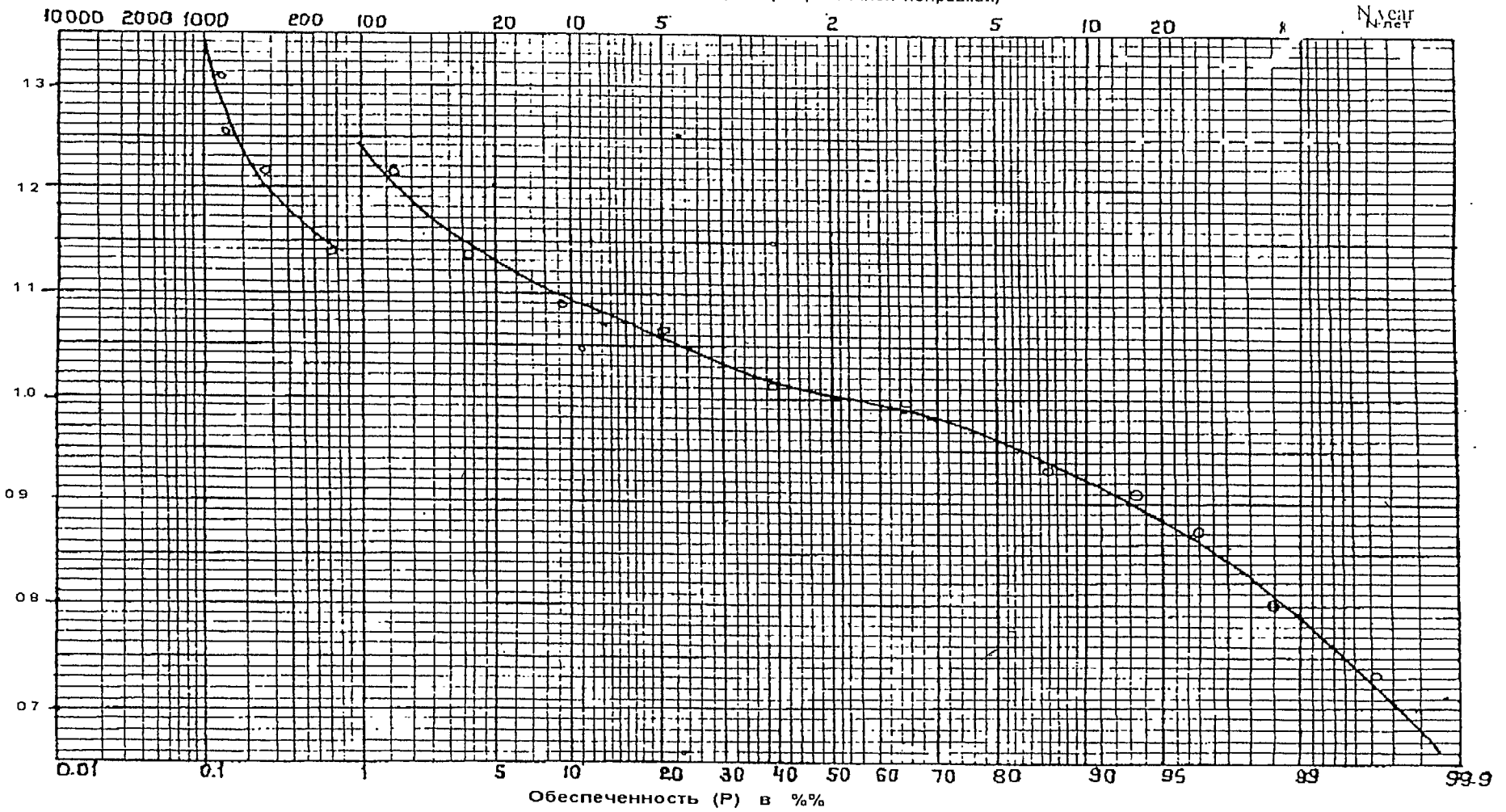

Probability (P) %%

Fig. 1

The strong and continuous winds cause dust storms in the region, when wind and deflation reach maximum intensity. The average number of days with a dust storm decreases from 32 in Muinak in the north to 4 in Nukus in the south. During the period March – June, more than 60% of dust storms are observed on the average within a year. The general duration of winds with a velocity of 3 $m.s^{-1}$ for example, at Muinak station, is 5540 hours/year, and 5 $m.s^{-1}$ – 2920 hours. Frequency of dust storms with a duration from 1.5 up to 5 hours (Table 6) is greatest.

Table 6. Frequency (%) of dust storms of various duration (hours) at Muinak station.

Duration (hr)	III	IV	V	VI	VII	VIII	IX	X
≥ 1	4	19	15	20	20	18	13	8
1,5-5	45	46	42	53	49	42	52	36
5,5-10	29	1	26	18	21	30	20	27
10,5-15	10	8	11	5	7	4	8	23

This duration (1.5-5 hours) prevails above other durations for all months of the year in which the dust storms take place. As is known, wind velocities, as well as other meteorological elements, suffer a great spatial variability. It means that the extrapolation of the data from a station to a sizeable distance is impossible without special examination or without definition of an error of such extrapolation. The need for an extrapolation of parameters of a wind is rather great since the objects of protection from atmospheric depositions or deflation might be situated at some distance from meteorological stations.

The method to be applied is that of correlation functions with the use of all volume of actual observations behind a wind in the southern Aral region. However, it is necessary to estimate statistical uniformity of numbers of observations. For this purpose the criterion of the consent α^2 is used. The important advantage before other criteria is that it can be applied to the empirical data with any law of distribution (4). The calculation of criterion of the consent was made using the formula (5):

$$\alpha^2 = n_1 x n_2 x \sum_{i=1}^{k} \left\{ 1 / (m'_i + m''_i) \times (m'_i / n_1 - m''_i / n_2) \right\}$$

Where: n_1 and n_2 – two independent samples of volumes located in 1 group with number m. The initial data were served with a series of observations on 7 couples of meteorological stations and stations located at various distances from each other.

As the values of criteria, α^2 under the table of distribution at probability $P(\alpha^2) = 0.05$ in all cases, have appeared below actual on the average on 10% (12.6 against 13.9), the modular transformation $V = Vi/\overline{V}$ is used at which were correlated not absolute, but normalized values of wind velocities. Such technique method allows to exclude influence of the local factors, for example, obstacles, specific only to the given station, to a wind flow. Factor of correlation, as criterion of narrowness of communication two variables, is calculated under the formula:

$$r(V_1,V_2) = \pm \frac{\Sigma(V_{i1} - \overline{V}_1)(V_{i2} - \overline{V}_2)}{\sqrt{\Sigma(V_{i1} - \overline{V}_1)^2 \times \Sigma(V_{i2} - \overline{V}_2)^2}}$$

In a considered case, particular expression of a correlation function is the profile of change of factor of correlation of the normalized values of wind velocity in the same moment of time, but at various distances between meteorological stations (Figure 2).

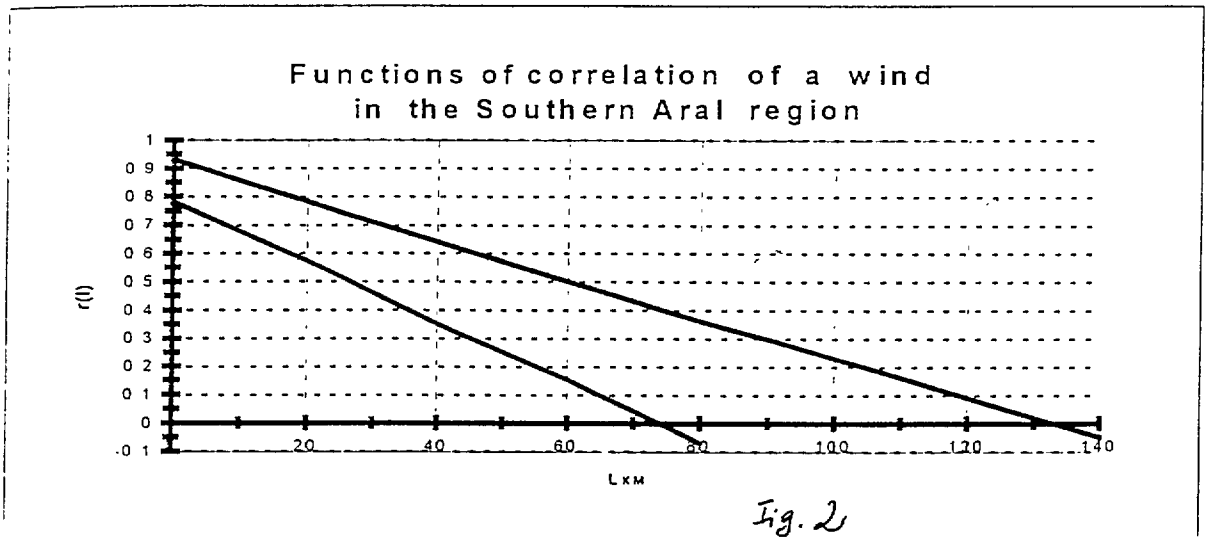

Fig. 2

The profile corresponds to May, when the wind activity in the region is most intensive, but can be constructed also for other months of the year. From Figure 2, it is visible that the statistical structure of a field of mean and greatest wind velocities is not identical, and indicates decrease of correlation functions with distance. So radius of correlation, i.e. distance, on which ordinate correlation decreases in time, with reference to

mean wind velocities is equal to 180 kms, and the greatest wind velocities have a radius of correlation of 250 kms.

The received correlation functions are expressed by the analytical formula:

$r(l) = r(o) - al$,

where $r(l)$ – factor of correlation at distance l between meteorological stations; r(o) – value of an empirical correlation function at $l \approx 0$, determined by a method of an extrapolation, a – structural parameter.

It is important to note that parameter r(o) essentially differs from unit even for mean wind velocities (Figure 2), that objectively testifies to presence of structural errors as a result of measurements in nature.

Disposing a correlation function, it is possible to determine a required mean quadratic error of an extrapolation of parameters of a wind on preset distance with the help of an equation: $E = \sigma\sqrt{1-[r(l)]^2}$; $P_{\%} = E/\overline{V}$

Where E – mean quadratic error of an extrapolation, $m.s^{-1}$; σ=Cv(V).

$\overline{V}$ - standard deviation $m.s^{-1}$; $r(l)$ – parameter of a correlation function;

P – relative error of an extrapolation.

The results of calculations are shown in Table. 7.

Table 7. Relative errors (%) of an extrapolation of mean and maximum wind velocities in the southern Aral region.

Parameter	Distance, km									
	1	3	5	10	15	20	25	30	40	50
$\overline{V}$	2,3	2,9	3,3	3,9	6,1	10,2	15,4	22,7	49,9	71,0
V_{max}	2,9	4,2	7,9	12,3	19,0	31,4	60,1	89,0	105	149

References

1. Protection of Agricultural Grounds and Environments. Minsk, 1984, 272 p.

2. Tursunov, A.A. The Aral Sea both ecological situation in Central Asia and Kazakhstan. Hydraulic Engineering Construction, Nol 6, 1989, p. 15-49.

3. Harsman, L.B., Zahidov, R.A., Rudak, M.S. Wind and power resources of Central Asia. Tashkent, 1994, 124 p.

4. Rojdestvenskiy, A.V., Chebotarev, A.N. Statistical methods in hydrology, Gidromeizdat, 1974, 423 p.

5. Smirnov, N.V., Dunin-Barkovskiy, L.V. A course in the theory of probabilities and mathematical statistics. "Science" Publishing House, 1965, 511 p.

Roses of wind

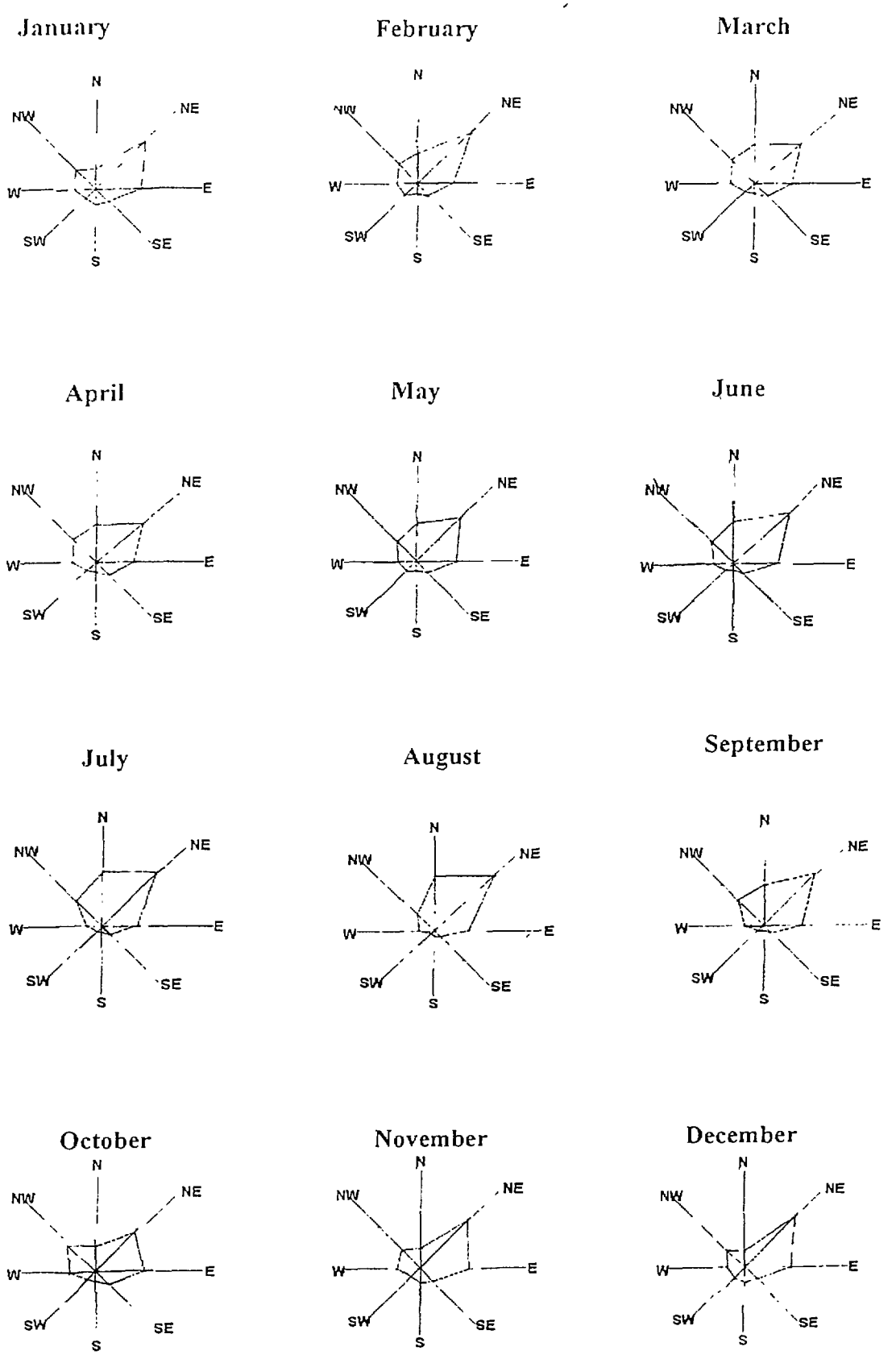

Fig. 3

PROTECTION OF INDUSTRIAL OBJECTS OF KUNGRAD DISTRICT FROM HARMFUL ACTION OF ATMOSPHERIC DEPOSITIONS.

Kungrad City and the industrial objects located in its vicinities, are situated within a zone of intensive irrigation. At the same time, in the north, northeast and northwest, the region is adjoined by extensive areas of so-called "swampy solonchaks" (Fig. 1). These, during diverse periods of the year can become a source of deflation into the atmosphere. It is clear that other surfaces in the Aral region too, for example the dried bottom of the Aral Sea, can serve as sources.

The "swampy solonchaks" are wet, because they periodically are intensively moistened and from this point of view can be divided into the following two types:

Type I – moistening by precipitation and condensation of air humidity,

Type II – moistening by precipitation, condensation and irrigational drainage water.

Irrespective of type of solonchak, its surface during the year changes from saturated with water to dry solonchak with high potential hazard of deflation of thenardite and other minerals and its deposition in other areas. It is therefore necessary to evaluate the moisture regime in the upper horizons of solonchak during an annual cycle. Losses of water from solonchaks is through evaporation and drainage. The evaporation from a water surface on a solonchak, equal in this case to potential evaporation, was calculated using the following formula:

$E_0 = an\,(e_0 - e_{200})\,(1 + bV_{200})$ .....(1),

where:

a and b - numerical parameters determined at processing of treatment empirical numbers (in this case, a = 0.14, b = 0.72),

e_0 – mean value of maximum elasticity of water vapor calculated at temperature of the surface of water (mb);

e_{200} – mean value of elasticity of water vapor (absolute humidity of air) at the altitude 2m above a water surface (mb), determined using the data of the meteorological station "Kungrad";

V_{200} – mean value of wind velocity at the altitude of 2m above a water surface ($m.s^{-1}$);

n – number of day during interval of time

For calculation of value V_{200} observations from "Kungrad" station are used:

$V_{200} = V_f G$,

where:

V_f – wind velocity at the altitude of the weathervane;

Fig. 2 **Soil & Land Use Maps of Aral Research Area**

25 km

Roses of wind (Kungrad)

Year

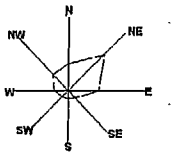

January

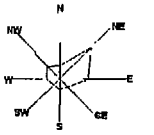

April

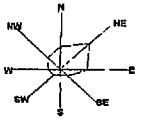

July

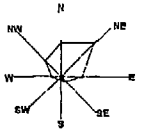

October

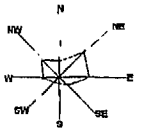

Swampy solonchaks

Tipical solonchaks

The salted grounds of the drained bottom of the Sea

Sands

Land use

100 Distribution of a deposition of salts in kg/hectare

G – complex factor taking into account logarithmic law of change of wind velocity with altitude above surface and also degree of protection of meteorological station.

The calculated sums of potential evaporation together with the information on precipitations (Table 1) allow to define time necessary for elimination of a layer of water above solonchak.

Table 1. The mean sums of precipitation (Xmm), potential evaporations (E_0mm) and their ratio.

Months / Element	I	II	III	IV	V	VI	VII	VIII	IX	X	XI	XII	Year
X_{mm}	10	10	18	16	11	7	3	3	2	6	10	12	108
$E_{0\,mm}$	40	52	75	85	120	145	160	130	90	55	48	40	1040
X/E_0	0.25	0.19	0.24	0.19	0.09	0.05	0.02	0.02	0.02	0.11	0.21	0.30	0.20

The mean sums of meteorological elements are suitable for use for one year, close to mean of the hydrothermal conditions.

For any year of design probability the factors of variation of precipitations Cv(X) = 0.42, evaporability $CV(E_0) = 0.10$, their differences $CV(E^0\text{-}X) = 0.14$ are calculated. Now it is obviously possible to define (determine) modular factors of a difference E_0-X, which is directly proportional to velocity of flowing of a layer of water on solonchak (Table 2).

Table 2. Modular factors of a difference (E_0-X) at preset probability.

Proba-bility %	1	3	5	10	25	50	75	90	95	97	99
Factor	1.23	1.19	1.16	1.13	1.07	1.00	0.93	0.87	0.84	0.81	0.77

When the layer of water covering it is removed from the solonchak, there comes a stage of evaporation from the soil surface.

In the beginning, the moisture of the soil corresponds to saturation, when all pores are filled with water except for trapped air. It has been shown (2) that in the interval from saturation up to field capacity, the evaporation is maximum and equal to potential evaporation Hence, for this interval are applicable the model and results obtained for the stage of flooding of the solonchak. The calculation is conducted for a layer of soil 0-5 cm. This layer is most dynamical, it is quickly moistened and quickly loses water. Water supply from lower horizons or the soil can be neglected because potential evaporation all year essentially surpasses the sum of precipitations (Table 1). Only intensive and continuous precipitation can reach equal potential evaporation and even exceed it. A layer of soil 0-5 cm quickly drains to the moisture of field capacity (GCT) and evaporation from the lower laying soil horizon, where W>Wgct, occurs in soil air.

When all water above field capacity drains ($W<W_{fc}$), progressive drying out of the soil occurs by the exponential law. For this period, the evaporation is calculated using the formula

$E_t = E_h e^{-zt}$.....(2),

where:

E_t – intensity of evaporation at the moment of time t;

E_h – intensity of evaporation in the initial moment, when was justified an inequality $W < W_{fc}$;

t – duration of a preset interval;

z – numerical factor.

The calculation of continuous evaporation under formulas (1) and (2) allows to reconstruct approximately the annual course of the moisture regime of a layer of soil 0–5 cm thick of a solonchak at various types of wetting (Fig. 2). In the figure, the categories of moisture of soil (soil-hydrological constants) are specified: full moisture capacity (MC), field capacity (FC), moisture of a gap of capillary tubes (GCT), wilting point (FW) and maximum hygroscopicity (MH).

Knowing the moisture regime of the soil, it is possible to evaluate the degree of hazard of deflation with reference to any period within the year. According to Figure 1, swampy solonchak of type I represents a source of highly dangerous deflation (mainly of thenardite) for the period of 6 months in a year. Solonchaks of type II are a source of high deflation hazard only for 2 months in a year and are safe for 5 months. As to solonchaks of type I, they are safe only 3 months in the year. The obtained data suggest that the method of struggle with deflation is by transfer of all areas to solonchaks of type II. However, this method requires the availability of significant volumes of water so necessary for the Aral Sea area.

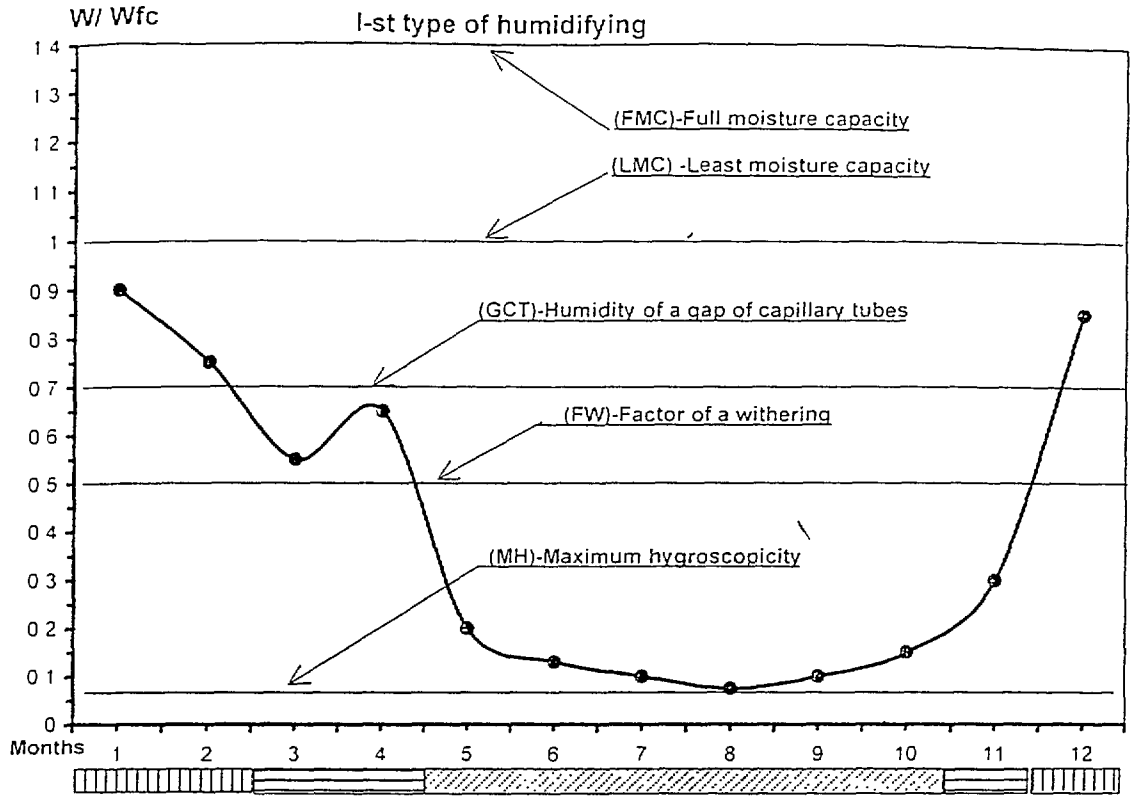

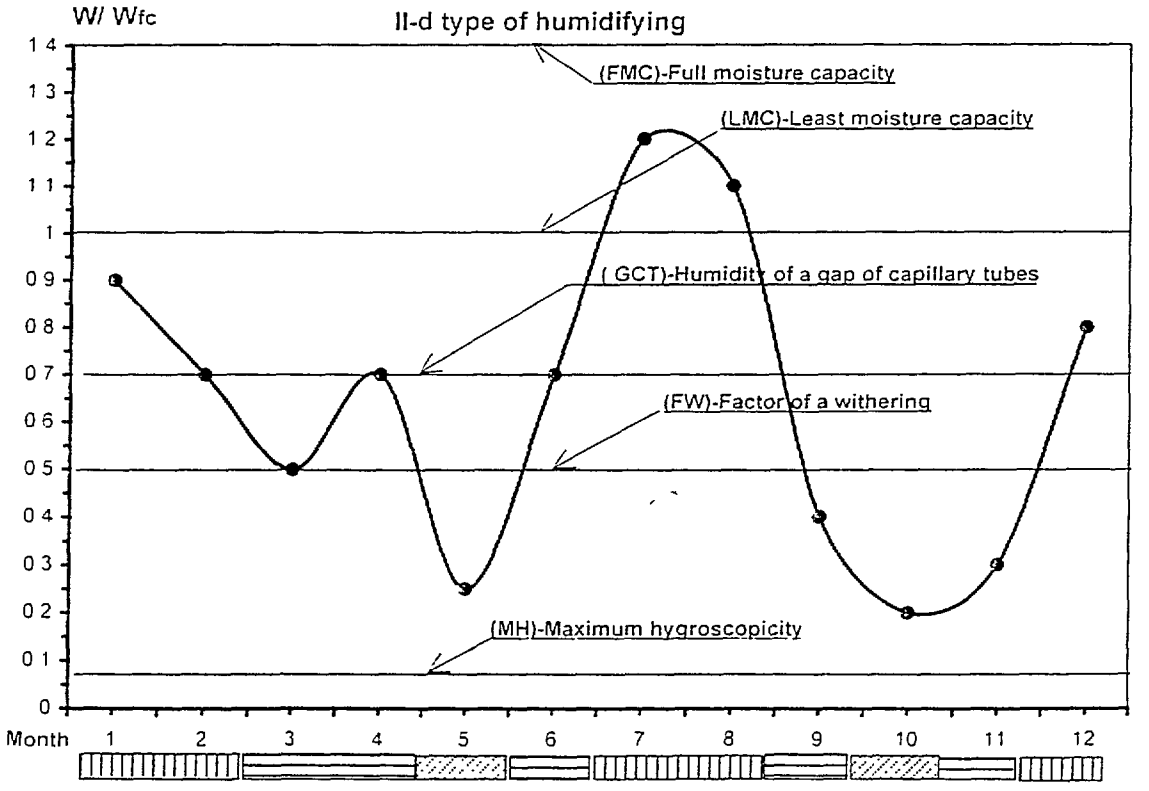

Hazard of deflation:

-high -mean -low

Figure 2. Annual cycle of moisture regime of soils under Solonchak Type I and Type II.

Moreover, reduction of irrigated areas in the region is expected and, as a result, the area of solonchaks of type I will increase and the area under solonchaks of type II will be reduced.

It is necessary to point out that even in those periods when the degree of hazard of deflation is high, not all areas of the solonchak will generate deflation material. The exception is made by those parts of the area which remain covered by water surfaces as a result of local topography. Such an area, for example, is Lake Mashankul (Fig. 1). For an estimation of the operational area of solonchak, which would be the object of melioration, large-scale maps are used.

As a result, it was possible to receive the relation:

$f/F = f(T)$,

where:

f - operational part of the area of solonchak during deflation;

F – general area of solonchak; T = time

Table 3. The area of deflation (f) in parts from the general area of Solonchak (F).

Type of humidifying	I	II	III	IV	V	VI	VII	VIII	IX	X	XI	XII
I	0	0.2	0.5	0.5	0.7	0.8	0.9	0.9	0.9	0.9	0.8	0.7
II	0	0.2	0.4	0.4	0.3	0	0	0	0.3	0.6	0.5	0.5

References

1. Instruction on calculation of evaporation from a surface of reservoirs. Hidrometeoizdat, Leningrad, 1989.

2. Poberejsky, L. Water Balance of the Aeration Zone During Irrigation. Hidrometeoizdat, Leningrad, 1987, 160 pp.

C) Scientific Impact of Collaboration

The impact of collaboration during the third project year was reflected in two visits of the collaborator partners from Uzbekistan in Israel, and in the participation of two of the Israeli investigators at international conferences.

The visits of the Uzbek partners in Israel had as their purpose discussions of the results obtained to-date and of the plans for further collaboration. A PC purchased in Israel for the Uzbek partners was taken back by them during their first visit. The computer had been loaded with programs for the modeling and GIS data. One of the Uzbek partners (Dr. M. Gilenko) was trained in the operation of the PC (Gateway product) and the programming.

Prof. Y. Mahrer presented a paper entitled: "Dust propagation following desiccation of the Aral Sea" at the international workshop on "Mineral Dust" held in Boulder, Colorado during June 1999. The paper was co-authored by E. Weinroth from Israel and M. Gilenko from Tashkent.

D) Description of Project Impact

Through the presentation of two papers at international conferences in Germany and the USA, the international scientific community become familiar with the research project, and contacts were established with other research groups carrying out research in Central Asia. One contact is with a group from Germany that works on bioremediation in the Aral Sea region. Another contact is with a group from the USDA-Agricultural Research Service in Lubbock, Texas, that works on the assessment of wind erosion. The research partners in Tashkent, Uzbekistan, were approached by the local authorities to evaluate dust hazards in the Kungrad area, western Amu Darai River Delta. For this area, industrial developments are planned.

E) Strengthening of Developing Country Institutions

In February 1998, a Gateway PC was transferred to "Waterproject" Tashkent, the partner Institution in Uzbekistan. Together with the PC, a program for dust transport modeling was transferred too. Also transferred were the GIS data pertaining to landforms in the Amu Darai River Delta, including soil types and land use. PC and programs, handled by the personnel that had been trained in Israel in 1998, should allow the partner Institute in Tashkent to further process the data and use the model for the solution of environmental problems currently arising.

F) Future Work

Emphasis in the fourth research year will be placed on the erodibility of the soil/sediment samples that had been brought to Israel from the Amu Darai River delta. These examinations had not commenced during the third project year because of difficulties encountered in the operation of the equipment. In addition to the soil samples brought back from the Aral Sea region in 1998, some more samples from near the settlement of Kungrad and from the recently dried-up bottom of the Aral Sea, will be made available. Parallel to these activities, modeling of dust transfer will be continued. Among others, the effects of several scenarios for the continuing desiccation of the Aral Sea will be examined. For the implementation of these portions of the project, an extension of the research duration for an additional year has been requested.

Section II

A) and B)

Difficulties in the transfer of funds to the Uzbek partners have continued in 1999, due to the extremely high inflation rate in that country. As a result, salaries for the Uzbek partners have not yet been transferred. On the other hand, outstanding debts have been settled. Communications with the partner Institute, Vodproject, are still problematic. It is anticipated that severe logistic and bureaucratic problems will jeopardize the operation of the field trial in the Aral Sea area.

D) Collaboration during 1999.

Collaboration with the partner institute in Uzbekistan in 1999 consisted primarily in two visits of the PI from Tashkent in Israel. During the first visit in February, a PC was delivered to the partners. Dr. M. Gilenko was instructed in the use of the model program for dust transfer, and in the use of the GIS cartographic data.

The second visit, in November, had as its purpose discussions on the deflatability studies to commence in Rehovot, Israel. The equipment to be used in these studies (wind tunnel and high volume impacter) was shown to the partners. Plans for the 4th research year were discussed.